Numerical analysis of multiphase flow over a square ribbed rough surface in an open channel

A Thesis submitted

In Partial Fulfilment of the Requirements
for the Degree of

Master of Engineering in Mechanical Engineering

By

Rajeev Kumar

Registration No- 154319 of 2020-21

Examination Roll No- M4MEC22020

UNDER THE GUIDANCE OF

Prof. Debasish Roy
&
Dr. Nitesh Mondal

JADAVPUR UNIVERSITY

DEPARTMENT OF MECHANICAL ENGINEERING

FACULTY OF ENGINEERING & TECHNOLOGY

JADAVPUR UNIVERSITY 188, RAJA S.C. MULLICK ROAD,
KOLKATA-700032, INDIA JULY, 2021

AUGUST, 2022

DECLERATION OF ORIGINALITY AND COMPLIANCE OF ACEDEMIC ETHICS

I hereby declare that the thesis entitled **"Numerical analysis of multiphase flow over a square ribbed rough surface in an open channel"** contains literature survey and original research work by the undersigned candidate, as a part of his MASTER OF ENGINEERING IN MECHANICAL ENGINEERING studies during academic session 2020-2022. All information in this document have been obtained and presented in accordance with the academic rules and ethical conduct. I also declare that, as required by these rules of conduct, I have fully cited and referenced all the material and results that are not original to this work.

Name: Rajeev Kumar

Examination Roll Number: M4MEC22020

University Registration Number: 154319 of 2020-21

Thesis Title: **Numerical analysis of multiphase flow over a square ribbed rough surface in an open channel**

Date: _____

Signature: _____

CERTIFICATE OF RECOMMENDATION

This is to certify that the thesis entitled "**Numerical analysis of multiphase flow over a square ribbed rough surface in an open channel**" is a Bonafide work carried out by Rajeev Kumar under our supervision and guidance in partial fulfilment of the requirements for awarding the degree of Master of Engineering in Mechanical Engineering under Department of Mechanical Engineering, Jadavpur University during the academic session 2020-2022.

Prof. Debasish Roy
Professor
Department of Mechanical Engineering
Jadavpur University, Kolkata
700032

Dr. Nitesh Mondal
Assistant Professor
Department of Mechanical Engineering
Ghani Khan Choudhury Institute of Engineering & Technology, Malda
732141

Prof. Amit Karmakar
Head of Department
Department of Mechanical Engineering
Jadavpur University, Kolkata

Prof. Chandan Mazumdar
Dean
Faculty of Engineering and Technology
Jadavpur University, Kolkata

CERTIFICATE OF APPROVAL*

The foregoing thesis, entitled "Numerical analysis of multiphase flow over a square ribbed rough surface in an open channel" is hereby approved as a creditable study in the area of CFD carried out and presented by **Mr. Rajeev Kumar (Registration No. 154319 of 2020-21)** in a satisfactory manner to warrant its acceptance as a prerequisite to the degree for which it has been submitted. It is notified to be understood that by this approval, the undersigned do not necessarily endorse or approve any statement made, opinion expressed and conclusion drawn therein but approve the thesis only for the purpose for which it has been submitted.

Final Examination for Evaluation of the Thesis

Board of Members

---------- ----------

---------- ----------

---------- ----------

*Only in case the thesis is approved

ACKNOWLEDGEMENTS

I would like to express my sincere and heartiest gratitude to my supervisor Prof. Debasish Roy and Dr. Nitesh Mondal for always having my back and showing me the right path to carry out this research work. He gave me confidence and filled me with enthusiasm regarding this research work. It was during our first discussion I was introduced to “Fluid flow in open-channel” for the “first time” and the way he explained the research area caught my attention and interest and it’s been more than a year since then and I thoroughly enjoyed what I did. I had always looked forward towards research as having the perfect balance between studies and enjoying life and I enjoyed the work-life balance under his guidance to the fullest. I am also thankful to him for providing me with support and assistance in every possible way and most importantly the friendly companionship we shared. I hardly had to wait a day before getting help from Sir which I had asked for in priority.

I would also like to mention my parents as their never-ending support and wholehearted helps are the real impetus to produce my best.

RAJEEV KUMAR
Jadavpur University

Date: _____

ABSTRACT

The work presents a numerical study on the characterization of the effect of turbulence of different properties over a rough bed. The model roughness comprised of periodically positioned, transverse square ribs that extended across the whole width of the channel. Different roughness is created on the bottom surface of the channel. We also know that sudden change of bed condition is frequent in an open channel flow. Change of bed condition affects the turbulence characteristics. In this literature, three types of roughness model namely k-type, d-type and intermediate roughness is used. Ribbed surfaces are widely used to enhance mass and momentum transfer in many applications. The mean flow and turbulent quantities vary quite significantly within the cavity as reported by many researchers over other geometries, and it appears the outer flow interacts more strongly with k-type roughness than d-type and intermediate roughness. Wall roughness also led to higher turbulence levels in the outer region of the boundary layer. The outer flow almost rides over the roughness layer in d-type roughness, with separation eddies confined to the gaps between the ribs. The mean separation zone for intermediate roughness, between d-type and k-type, is about the same size as the cavity between the ribs, but the outer flow is impacted by enormous turbulent eddies emerging from the roughness layer. When two consecutive ribs separate and reconnect, significantly larger and more frequent eddies are thrown into the outside flow, resulting in substantial interaction between the roughness layer and the outer flow. The effect of velocity of upper layer fluid is considered in this study to see the influence of velocity on the lower fluid or in the intermediate zone of two fluids.

Table of Content

List of Figures

Figure

List of Tables

Tables

Chapter 1: Introduction

1.1. Introduction

The turbulent flow at high Reynolds number over a rough surface is common in nature and is used in a variety of practical flows. As a result, many researchers have studied the hydrodynamics of rough bed flows extensively over the last few decades, and they have discovered differences in the structure of turbulent flow over smooth and rough surfaces close to the wall or roughness elements. Understanding the flow characteristics over two-dimensional periodic rib roughness with different roughness configurations has received a lot of attention for understanding rough bed flows, which is useful in a lot of engineering fields. Changes in the pitch separation (P) of a rough surface resulting from a series of two-dimensional (2D) elements (such as ribs), for example, influence the turbulent flow characteristics.

Perry et al. [1] discovered this and classified roughness as d- and k-type based on the pitch to roughness height ratio (P/k), with $P/k < 5$ considered d-type, $P/k > 5$ considered k-type, and $P/k = 5$ considered intermediate roughness. These roughness configurations are frequently used in hydraulic engineering applications to reduce velocities by generating a series of hydraulic jumps as a means of energy dissipation. Rough surfaces like this are commonly used to improve heat transfer. More generally, they are also of prime importance for furthering the fundamental science and understanding of flow over any rough boundary.

Open-channel flow is a type of channel flow in which a liquid is exposed to a gas. The most common liquid is water that has been exposed to atmospheric air. Flow in open channels is typically driven by gravity, as opposed to pipe flow, which is frequently driven by pressure gradients.

Turbulent flows over smooth surfaces have long been studied, both experimentally and theoretically. Experimentally, the importance of the wall layer was convincingly demonstrated. Much more detailed information is now available thanks to the introduction of direct numerical simulations (DNS). The mechanisms involved in the generation of self-sustaining turbulent motion near the wall are now well understood, and the communication between the inner and outer layers has been elucidated using this research tool.

Despite its importance in industrial applications, flows over rough surfaces are poorly understood. In the limit of infinite Reynolds numbers, all real surfaces behave as rough walls, and the details of the wall can have a significant impact on the flow characteristics. The impact of altered surface topography on the mean velocity profile has been well documented or reviewed. The roughness of the wall is commonly assumed to be a local effect that only affects the inner layer up to a distance of about 4 to 5 roughness heights. Because the roughness elements in this roughness sublayer will interact strongly with the streamwise vortices found near the walls, the inner region is expected to be significantly modified compared to a smooth wall.

The assumption that the wall effect is limited to a certain number of roughness element heights leads to the argument that in the fully rough case the inner layer should be modified from the smooth wall relation

$$U^+ = 1/\kappa \ln y^+ + A \qquad 1.1$$

to the form

$$U^+ = 1/\kappa \ln(y/k) + B(k^+),\ B(k^+) = A - \Delta U^+ + 1/\kappa \ln k^+, \qquad 1.2$$

where U is the mean velocity in the streamwise direction, y is the distance from the surface and κ is the von Karm‘an constant. A is the smooth wall constant and ΔU^+ is the modification of this constant due to roughness effects and is frequently called the ‘roughness function’. In this work, it can be distinguished the effect of different type of roughness in case of fluid flow referred here namely d-type, intermediate type and k-type. The roughness function for fully rough flow is a function of the length of scale ε for both 'k' and 'd' type. The ε can be expressed as distance below the crests of the elements that the effective wall of the boundary layer. One effect of surface roughness is to increase momentum transfer and flow resistance. For d-type roughness, the cavity is found to comprise two principal vortices of opposite rotation, rather than a single principal vortex of clockwise rotation that might be expected for lid-driven cavity flow [8]. The DNS simulations similarly indicate the cavity of d-type roughness to be occupied by a large recirculation region with a significant secondary vortex, of opposite rotation, toward the lower upstream corner of the cavities [21].

1.2. Objective of the thesis

Study about the fluid flow in open channel is a classical problem in fluid dynamics and it has been studied over the year for many types of rough surface. One of the main difficulties when studying rough-wall flows is the reliable determination of the effective wall shear stress. From past many years many studies have been done on this topic with different type of roughness. This study includes square rib for creating roughness, and the distance between two consecutive rib defines the type of roughness. The main objective of this thesis is that to visualize the wall shear stress and impact of force on the brick surface for different type of roughness pattern while changing the mean stream velocity. So that it can be understandable that the flow pattern of the flowing fluid and intensity of the turbulence of the flow path over the rib surface in an open channel.

1.3. Thesis structure

This chapter consists of introducing the present study. And it also contains the objectives of the thesis work. The reader is then introduced to the main contents of the following chapters. Chapter 2 discusses the details of literature review.

Chapter 3 discusses the fundamental equations describing the open channel fluid flow. The middle part of this chapter also discusses the principles of the CFD. Further, it contains the different type of methods used and some the equations solved during the simulation. And this chapter also include the properties of multiphase used in this thesis. The main content of this chapter is about the volume of flow methos, named selection used and the type of meshing used in this simulation.

Chapter 4 includes the results part for the case 1(when velocity is given to only water) and it also contains the velocity contour, plot of wall shear stress on vertical height of brick and the variation of velocity just after the brick for different type of roughness used in this thesis.

Chapter 5 includes the results part for case 2 of my study (when velocity is given to both water and air above it). This chapter again includes the contours and plots of velocity od wall shear stress respectively for different type of roughness used.

Chapter 6 concludes the whole thesis. It focuses on the significant finding from the theory and future scope of study.

Chapter 2: Literature review

2.1. Literature Review

Perry et. el. [1] describes in this paper a detailed experimental study of turbulent boundary-layer development over rough walls in both zero and adverse pressure gradients. In this study two distinct wall roughness geometries were chosen, k-type roughness and d-type roughness, each with a different rule of behaviour; they were chosen based on their reported behaviour in pipe flow studies. However, results for both types of roughness have been found to correspond with a Reynolds number based on the wall shear velocity and the distance below the crests of the elements from which the logarithmic distribution of velocity is recorded. It appears that two major forms of roughness, denoted here as 'k' and 'd,' can be separated. The Nikuradse-Clauser correlation approach is used for 'k' type roughness. This correlation technique does not apply to 'd' type roughness, which is characterised by depressions or narrow lateral grooves in the wall. Nakagawa et. el. [2] studied the Influence of a wavy boundary on turbulence on rough surface. They are comparable in that significant quadrant 2 occurrences in the outer flow are associated with plumes that arise from the wall region and spread over long distances in both cases. For flat and wavy surfaces, measurements of the skewness of the streamwise and wall-normal velocity variations, as well as quadrant assessments of the Reynolds shear stresses, are qualitatively equivalent. The skewness magnitudes and the ratio of quadrant 2 to quadrant 4 contributions, on the other hand, are bigger for the wavy surface. Thus, there is evidence that turbulent patterns are universal in the outer flow, as well as quantitative variances in statistics reflecting differences in how the fluid interacts with the wall. Pokrajac et. el. [3] studied about the Quadrant analysis of persistent spatial velocity perturbations over square-bar roughness, He Consider an unique application of the quadrant approach in the context of the double-averaged Navier-Stokes equations for examining open channel flow near rough beds. It is well known that flows in channels with rough beds have different mean velocity profiles compared to flow over smooth beds, because of considerably larger drag. Hirt et. el. [4] studied about the Volume of fluid (VOF) method for the dynamics of free boundaries. Several strategies have previously been employed in finite difference numerical simulations to approximate free borders. A simple yet powerful method based on the concept of a fractional volume of fluid is given (VOF). This method is demonstrated

to be more flexible and efficient than existing methods for dealing with complex free boundary setups. It is common to use only one value for each dependent variable characterising the fluid state in each cell of a mesh. As a result, the use of multiple points in a cell to define the region occupied by fluid appears unnecessary. However, suppose we define a function F with a value of unity at any place occupied by fluid and zero otherwise. The average value of F in a cell would then represent the fractional volume of fluid in the cell. A unit value of F, for example, would equate to a cell full of fluid, whereas a zero value would imply that the cell held no fluid. Manes et. el. [5] studied Turbulence structure of open channel flows. It is difficult to understand the behaviour of turbulent open channel flows across permeable surfaces. It is unclear, in particular, how the surface and subsurface flow inside the permeable substrate interact and impact one another. To address this issue, he conducted two sets of experiments: one including velocity measurements in open channel flows over an impermeable bed formed of a single layer of spheres, and the other involving velocity measurements over and within a permeable bed composed of five similar layers. Velocity measurements were taken in open channel flows over and within a permeable base of five layers of beads. The comparison of flow statistics with an impermeable bed comprised of only one layer of such beads allowed researchers to investigate the impact of permeability on surface flow statistics. Velocity measurements within the five-layer bed allowed researchers to investigate the turbulence qualities of the subsurface flow and its interaction with the surface flow above. Raushan et. el. [6] Studied about the turbulent flow characteristics over ribbed surface in presence of unidirectional wave over steady current. he used the model roughness comprised of periodically positioned, transverse square ribs that extended across the whole width of the channel. he also concluded that ribbed surfaces are widely used to enhance mass and momentum transfer in many applications. Ferreira et. el. [7] Studied about the CFD modelling of rough bed open channel flow. He also said the relative magnitude of the double-averaged quantities is strongly dependent of the bed layout. k-ε transport of the turbulent kinetic energy seems to be a manifestation of the near wall modeling approach. Balachandar et. el. [8] Studied about the Effect of Reynolds Number on Wall-normal Turbulence Intensity in a Smooth and Rough Open Channel Using both Outer and Inner Scaling. He summarised that the change of bed condition affects the turbulence characteristics in both streamwise and wall-normal direction. Tachie et. el. [9] have studied the Rough Wall Turbulent Boundary Layers in Shallow Open Channel Flow. he states that the boundary layer

thickness was comparable with the depth of flow and the turbulence intensity in the channel flow. Wall roughness also led to higher turbulence levels in the outer region of the boundary layer. he also found a general conclusion of their study is that bed surface effects, in this case due to roughness, can influence the flow structure in the outer region of the boundary layer, which contradicts the wall similarity hypothesis. Finally, the fact that rough wall effects are not restricted to the inner region and that outer turbulence intensity penetrates deep into the wall region suggests that rough-wall flows in the presence of elevated turbulence intensities may be an ideal flow for studying the interactions between the inner and outer regions of the turbulent boundary layer. Agelinchaab et. el. [10] studied about the Open channel turbulent flow over hemispherical ribs and he also varied the pitch-to-height ratio is to achieve the so-called d-type, intermediate and k-type roughness. He used a particle image velocimetry to obtain detailed velocity measurements in and above the cavity. He also observed that interaction between the outer flow and the shear layers generated by ribs is strongest for k-type and least for d-type ribs and their results also show that hemispherical ribs are less effective in augmenting flow resistance compared to two-dimensional transverse ribs. The mean flow and turbulent quantities vary quite significantly within the cavity as reported in prior works over other geometries, and it appears the outer flow interacts more strongly with k-type roughness than d-type and intermediate roughness. Cassan et. el. [11] studied about the distribution of velocity in an open channel flow with spatially distributed roughness. He used a method based on the mixing length model and sub-division of the wetted surface, to modified easily and integrate a lateral distribution of roughness. He concluded that it is justified to use it in design process of hydraulic structure where the flow is unidirectional such as fish passes. Gandhi et. el. [12] studied about the investigation of flow profile in open channel using CFD. In this paper he discussed the effects of bed slope, upstream bend and a convergence / divergence of channel width on velocity profile and observed that the actual velocity profile differs from the normal profile due to non-existence of ideal flow conditions, and this should be taken care during the planning of measurement of velocity by any method in the flow section to evaluate the discharge using velocity-area integration technique. Nikora et. el. [13] studied about the spatially averaged open-channel flow over rough bed and he suggested in this paper that the double-averaged (in temporal and in spatial domains) momentum equations should be used as a natural basis for the hydraulics of rough-bed open-channel flows, especially with small relative submergence. In this paper he

considered the simplest case of 2D, steady, uniform, spatially averaged flow over a rough bed with flat free surface. He introduces the spatially averaged momentum equations, and using them, subdivide the flow into specific regions. McEwan et. el. [14] discussed the spatial averaging concept in environmental hydraulics and develop it further by considering transport equations for fluid momentum, passive substances, and suspended sediments. The suggested equations in this paper differ from those considered in terrestrial canopy aerodynamics and porous media hydrodynamics by accounting for roughness mobility, change in roughness density in space and time, and particle settling effects for the case of suspended sediments. he also showed that the suggested methodology offers better definitions for hydraulic parameters such as flow uniformity, two dimensionality, and the bed shear stress. He suggested the modelling approaches in hydrodynamics can be classified depending on temporal and spatial resolution as: 1. direct numerical simulation (DNS) with no averaging, 2. large eddy simulation (LES) with small scale spatial-averaging, and (3) time-averaged numerical simulation based on the RANS equations. Wen et. el. [15] summarised that the Bed shear stress is an important measure of benthic habitats since it is related to many ecological processes. In this study, he focused on the fluctuating characteristics of shear stress in rough-bed open-channel flows. From this study he tried to Improve Delayed Detached Eddy Simulation (IDDES) model to investigate the turbulent characteristics of near-bed flow, considering the balance between calculation cost and accuracy. In this study he used k-ε model. he found from this study that the total effect of the flow fluctuations exerted upon the object decreases with the increase in its length scale. In this study, he used numerical simulations to study shear stress characteristics over a natural rough riverbed, including the time-averaged and fluctuating characteristics. Djenidi et. el. [16] studied in this paper about the turbulent boundary layer over transverse square cavities. he used LDV measurements and flow visualizations were carried out in a turbulent boundary layer over two-dimensional square cavities placed in a transverse direction to the flow and spaced one cavity width apart in the x-direction. he suggested that outflows play a role in the mean energy production rate is consistent with the idea that the mechanism for sustaining the turbulence is closely related to the vorticity generation. He found that there is strong evidence of occurrence of outflows of fluid from the cavities as well as inflows into the cavities. These events occur in a pseudo-random manner and are closely associated with the passage of near-wall quasi-streamwise vortices and local maximum in the Reynolds shear stress is observed in the shear layers over the cavities.

Antonia [17] studied about the effects of surface roughness in turbulent boundary layer. They concluded that the effects of surface roughness on a turbulent boundary layer are examined by comparing results from a smooth wall boundary layer to observations from two rough walls. Although designed to create the same roughness function, i.e., to have nominally the same influence on the mean velocity profile, the two rough surfaces have drastically different surface geometries. They also observed that the surface geometry significantly affects the turbulent characteristics of the flow, even when roughness geometries are chosen so as to achieve nominally the same effect on the mean velocity. The statistics presented clearly demonstrate that simply analysing the influence of roughness on the mean velocity profile is insufficient to characterise it. Krogstad et. el. [18] studied about the experimental and numerical study of channel flow with rough walls. The mean flow follows the law of the wall for both surfaces and the velocity defect suggest that the outer layer is very little affected by the roughness. The rough wall profile is attenuated in the outer region, which is the opposite of what has been observed for a boundary layer. only one of the channel walls was roughened while the other wall remained smooth in this study. The present paper reports on a combined experimental and computational investigation in which laboratory measurements and DNS data obtained from the same rough channel configuration are examined. These measurements were performed in a closed return wind tunnel with a working section consisting of two parallel plates forming a rectangular channel. cui et. el. [19] studied about the Large-eddy simulation of turbulent flow in a channel with rib roughness. The spacing of the roughness elements is varied to reproduce the so-called d- and k-type roughness, and an intermediate roughness between the two. The outer flow almost rides over the roughness layer in d-type roughness, with separation eddies confined to the gaps between the ribs. The mean separation zone for intermediate roughness, between d-type and k-type, is about the same size as the cavity between the ribs, but the outer flow is impacted by enormous turbulent eddies emerging from the roughness layer. When two consecutive ribs separate and reconnect, significantly larger and more frequent eddies are thrown into the outside flow, resulting in substantial interaction between the roughness layer and the outer flow. in this paper he discussed an interesting result that It is commonly believed that for d-type roughness, the roughness function is related to the pipe diameter d (or channel height H, or boundary layer thickness d), and this is the reason why it is named d-type. Nagano et. el. [20] discussed about thermal fields in turbulent channel flow with transverse-rib

roughness. To investigate the effects of roughness on statistical quantities in the velocity and thermal fields, direct numerical simulations (DNS) of heat transfer in turbulent channel flows with transverse-rib roughness were performed by varying their spacing, width, and height, and turbulent heat transfer with k-type and d-type roughness walls were simulated. It is discovered that when ribs are arranged to facilitate turbulent mixing, the distributions of mean velocity and temperature become highly asymmetric. There are systematic changes in secondary flow patterns between ribs. The k-type roughness is observed to provide the best heat transmission performance. Leonardi et. el. [21] discussed about Structure of turbulent channel flow with square bars on one wall. They perform direct numerical simulation for organised motion in a turbulent channel flow with a succession of square bars on the bottom wall. Several values of the ratio w=k have been thoroughly investigated, where k is the bar height and w is the longitudinal gap between consecutive bars. The coherence decreases in the streamwise direction as w=k increases, with a minimum for w/k =7. This is because the outward motion occurs primarily near the leading edge of the components. Hyun Lee et. el. [22] discussed about measurement of heat/mass transfer with continuous and multiple V-shaped ribs in rectangular channel. The effects of aspect ratio on heat/mass transfer in rectangular channels with two different V-shaped rib configurations, which are continuous V-shaped rib configuration with a 60^{o}attack angle and multiple (staggered) V-shaped rib configuration with a 45^{o}attack angle, were investigated. The effect of channel aspect ratio was higher significance for the continuous 60^{o} V-shaped rib configuration than for the numerous 45^{o} V-shaped rib arrangement. Coleman et. el. [23] studied for Spatially Averaged Turbulent Flow Over Square Ribs. They perform series of experiment for fully rough turbulent subcritical flow over 2D transverse repeated-rib roughness of varying spacing $\lambda/h=1–16$ (roughness spacing/height ratio), with $h/H=0.09$ (roughness height/flow depth). Results from this study confirms the circulation patterns for the conceptual d-type and k-type roughness. For d-type roughness, the cavity is found to comprise two principal vortices of opposite rotation, rather than a single principal vortex of clockwise rotation that might be expected for lid-driven cavity flow. For closely spaced d-type roughness, stably separated vortices occupy the whole cavity between ribs with minimum disturbance of the outer flow. For widely spaced k-type roughness, reattachment occurs before the next rib, and eddies penetrating to the boundary-layer edge are shed from the roughness. A smooth transition from skimming d-type flow to interactive k-type flow occurs at rib spacing of $\lambda/h=5$ rib wavelength/height.

Chapter 3: Methods &Methodology

3.1. Fluid Mechanics - Governing Equations

Fluid Mechanics is the study of how fluids behaves when subject to forces. In general, the forces are split into two categories, body and surface forces, an example of a body force is the gravitational force, an example of a surface force is for instance shear forces caused by the wind blowing. The equations governing the fluid motions are the Navier-Stokes equations (3.1) and the continuity equation (3.2)

$$\frac{\partial u}{\partial t} + (u \cdot \nabla)u = -\frac{1}{\rho}\nabla p + F + \frac{\mu}{\rho}\nabla^2 u \qquad 3.1$$

$$\nabla \cdot u = 0 \qquad 3.2$$

where ρ is the density of the fluid, u is the velocity vector, p is the total pressure, F is the sum of the body forces and μ is the dynamic viscosity of the fluid. The Navier-Stokes equations are derived from the principle of conservation of momentum, the continuity equation is derived from the principle of conservation of mass.

3.2. Turbulence

In Fluid Mechanics there are several dimensionless variables that relates to different flow properties. One such number is the Reynolds number

$$R_e = \frac{\rho u L}{\mu} \qquad 3.3$$

where u is some representative velocity of the flow, for instance the bulk flow and L is some representative length scale for the flow. The Reynolds number is the ratio between inertial forces and viscous forces. The flow of the fluid can either be laminar or turbulent.

Whether the flow is laminar or turbulent is decided by the magnitude of the Reynolds number. For large Re the flow is turbulent, i.e., when the inertial forces are comparatively large to the viscous forces. Laminar flow is characterized by smooth streamlines and highly ordered motion. Turbulent flow, on the other hand, is characterized by chaotic three-dimensional velocity fluctuations and highly disordered motion [1].

3.3. Reynolds Averaged Navier-Stokes Equations

One common way to simplify the Navier-Stokes equations is to divide the velocity field into two parts, one mean component and one fluctuating random component

$$u(x,t) = \langle u(x,t)\rangle + u'(x,t) \tag{3.4}$$

Where $\langle u(x,t)\rangle$ is the time-averaged velocity and $u'(x,t)$ are the turbulent fluctuations. This is called the Reynolds decomposition. From this decomposition the Reynolds Averaged Navier-Stokes (RANS) equations follows.

In tensor notation the equation can be written as

$$\frac{\bar{D}\langle U_j\rangle}{\bar{D}t} = \vartheta\nabla^2\langle U_j\rangle - \frac{\partial\langle u_i u_j\rangle}{\partial x_i} - \frac{1}{\rho}\frac{\partial\langle p\rangle}{\partial x_j} \tag{3.5}$$

Where $\frac{\bar{D}}{\bar{D}t}$ is the mean-substantial derivative, ν is the kinematic viscosity and $\frac{\partial\langle u_i u_j\rangle}{\partial x_i}$ is the derivative of the Reynolds stress tensor. The mean continuity equation is

$$\nabla\cdot\langle u(x,t)\rangle = 0 \tag{3.6}$$

Equations (3.5) and (3.6) together describe the three-dimensional time-averaged velocity field. There are four different equations and five unknown variables, three velocity components, the pressure and the Reynolds stress. This is known as a closure problem, in order to be able to solve the set of equations the Reynolds stress needs to be modelled [5].

3.4. Flow over rough bed

For sufficiently uniform rough surfaces the implicit equation known as the Colebrook equation can be used

$$\frac{1}{\sqrt{f}} = -2\log_{10}\left(\frac{\epsilon/D_H}{3.7} + \frac{2.51}{Re\sqrt{f}}\right) \tag{3.7}$$

where ε is the mean height of the roughness and D_H is the hydraulic diameter and f is the friction factor, also known as the Darcy friction factor. The ratio ϵ/D_H is also known as equivalent sand-grain roughness because the initial experiments designed included surfaces where sand grains of known height had been glued to the walls.

3.5. Double-Averaged Navier-Stokes Equations

It has been suggested that for environmental hydraulics the conventional full roughness sub-grid representation approach is insufficient since the flow adjacent to the rough surface will always be non-uniform. One way to combat this problem is to perform a so-called double-averaging. Recall that the RANS equations are based upon time-averaging, with double-averaging one implies that the velocity components are averaged in both time and space.

A decomposition similar to the Reynolds decomposition, called the Gray's decomposition, can be used

$$u(x,t) = \langle \tilde{u}(x,t) \rangle + \bar{u}(x,t) \qquad 3.8$$

Where $\langle \tilde{u}(x,t) \rangle$ is the double-averaged velocity and $\bar{u}(x,t)$ are the spatial fluctuations. The double-averaged velocity is measured in a plane parallel to the mean flow. Averaging in space also introduces spatial fluctuations. These can statistically be modelled in a similar way as for the RANS equations. Unfortunately, this feature is not implemented in ANSYS CFX. It has been suggested that spatial averaging can be done post simulation and still be meaningful.

3.6. CFD – Computational Fluid Dynamics

The Navier-Stokes equations are highly non-linear partial differential equations and can't be analytically solved for the general case. One way to combat this problem is to discretize the Navier-Stokes equations, using for instance the finite difference method or the finite volume method to get a system of algebraic equations instead. These systems of equations can then be solved by using numerical methods.

Computational Fluid Dynamics also generally called CFD is an important branch of fluid mechanics and it uses numerical method and algorithms to analyse and solve fluid flow problems. It has become popular since the previous method, experiment and theoretical are either very expensive, time consuming, or involve too much labour. In CFD, computers are used to solve the algorithms that define and analyse the fluid flow. Due to increase in the computational capabilities over time and better numerical solving method most experimental and theoretical work has been done using CFD. CFD is not only most effective but it helps one analyse and simulate complex geometries, Heat transfer and shock waves in a fluid flow. It also helps solve PDE of any order in a fluid flow. CFD

mainly helps analyse the internal and external fluid flow. The use of CFD has become increasingly popular in branches of engineering such as Aerospace to study the interaction the propellers or rotor with aircraft fuselage, Mechanical to obtain temperature distribution of a mixing manifold, Bio-medical engineering to study the respiratory and circulatory system. There are a few simple generic steps that must be followed for CFD analysis.

- CFD is the simulation of fluid engineering system using modelling (mathematical physical problem formulation) and numerical method.
- CFD made possible by the advent of digital computer and advancing with improvements of computer resources.

CFD is the science of predicting fluid flow, heat and mass transfer, chemical reactions and related phenomena by solving numerically the set of governing mathematical equations,

- Conservation of mass, momentum, energy,
- Effects of body forces,

Why we use CFD:

- Analysis and design (simulation-based design instead of build and test,
- More cost effective and more rapid than Experimental Fluid Dynamics,
- CFD provides high-fidelity database for designing flow field,
- Full scale simulations,
- Environmental effects,
- Hazards (explosion, radiation, pollution).

Where CFD is used,

- Aerospace,
- Automotive,
- Biomedical,
- Chemical processing,
- HVAC,
- Marine,
- Oil & gas,
- Power generation,
- Sports

3.7. Physical principle of CFD

For all flows, ANSYS FLUENT solves conservation equations for mass and momentum. In this problem turbulent modelling is solved for open channel fluid flow on square rib rough bed. The open channel flow is modelled in FLUENT using volume of fluid (VoF) formulations. The flow involves existence of a free surface between the flowing fluid and the atmospheric air above it. The flow is generally governed by the forces of gravity and inertia. In VoF model, a single set of momentum equations is solved for two or more immiscible fluids by tracking the volume fraction of each of the fluids throughout the domain.

3.7.1. Methodology of CFD

In general, CFD simulations can be distinguished into three main stages, which are

- Pre-processor
- Solver
- Post-processor

3.7.1.1. Pre-Processor

Pre-processor consists of the input of the flow problem to a CFD program by means of an operator friendly interface and the subsequent transformation of this input into a form suitable for use by the solver. Computational domain, which is the fluid region to be analysed, is discretized in small elements called mesh. After the mesh generation, the properties of fluid are defined and appropriate boundary conditions is also specified.

3.7.1.2. Solver

Solver calculates the solution of the CFD problem by solving the governing equations. The governing equations of the fluid flow can be written in the two forms, i.e., the partial differential form and the integral form. Both these forms are complimentary to each other. The differential form can be obtained by from the integral form and vice versa. Partial differential equations (PDEs) consist of some flow variables like velocity, pressure and their derivatives. To solve the PDEs in a computer, they must be converted into algebraic equations and the process is called numerical discretization. Numerical discretization can be done in following ways as,

- Finite difference method (FDM)
- Finite element method (FEM)
- Finite volume method (FVM)

The finite difference method and the finite volume method are quite similar to each other as they both solve the governing equations at a point by using the neighbouring values of it. FDM is a differential approach as it discretizes the PDEs to get the strong form of the solution. On the other side, the finite element method is the most popular method among these due to its capability to simulate the complex geometries. It is an integral approach in which the weighted residuals of the governing equations are integrated and the weak form of the solution is obtained. FEM solves the equations for each element, indecently from neighbouring elements. Due to this, the whole flow domain is conserved. In the present work, the ANSYS Fluent 21R2 is used, which is based on the FVM.

3.7.1.3. Post-Processor

Numerical solution is obtained from the mathematical model by using the solver and selected variables are obtained at selected points. Everything else is constructed from these variables at selected points through a process called post- processing. ANSYS Fluent has a dedicated component for this, called CFD Post. In the CFD Post, the solution can be visualized in the form of contours of velocity or pressure, by plotting different quantities such as pressure coefficient, Wall shear stress.

3.8. Turbulence Modelling - The k-ε Model

There are several ways to model the Reynolds stress. Some commonly used methods are linear eddy viscosity models, algebraic models, one- and two-equation models and Reynold stress transport models (RSTM). The most commonly used turbulence model in industrial applications is the k-ε model. The k-ε model is based on the turbulent viscosity hypothesis. The k-ε model is a two-equation model that models two turbulent quantities, the turbulent energy dissipation ε and the turbulent kinetic energy k. From these two quantities a turbulent time-scale (3.9), a turbulent length scale (3.10) and the turbulent viscosity (3.11) can be defined,

$$T = \frac{k}{\epsilon} \tag{3.9}$$

$$L = \frac{k^{\frac{3}{2}}}{\epsilon} \tag{3.10}$$

$$\vartheta_t = \frac{C_\mu K^2}{\varepsilon} \quad 3.11$$

The transport equation for k is,

$$\frac{\bar{D}k}{\bar{D}t} = \nabla \cdot \left(\frac{\vartheta_T}{\sigma_k}\nabla k\right) + P - \epsilon \quad 3.12$$

Furthermore, the equation for ε can be written as,

$$\frac{\bar{D}\epsilon}{\bar{D}t} = \nabla \cdot \left(\frac{\vartheta_T}{\sigma_\epsilon}\nabla \varepsilon\right) + C_{\varepsilon 1}\frac{P_\varepsilon}{k} - C_{\varepsilon 2}\frac{\varepsilon^2}{k} \quad 3.13$$

where ϑ_T is the turbulent viscosity, P is the production rate of turbulent kinetic energy and $C_\mu = 0.09, C_{\epsilon 1} = 1.44$,$C_{\epsilon 2} = 1.92, \sigma_\varepsilon = 1.3$ and $\sigma_k = 1.0$ are model parameters [5].

3.9. Volume of fluid (VoF) method

It is common to use only one value for each dependent variable characterising the fluid state in each cell of a mesh. As a result, the use of multiple points in a cell to define the region occupied by fluid appears unnecessary. However, suppose we define a function F with a value of unity at any place occupied by fluid and zero otherwise. The average value of F in a cell would then represent the fractional volume of fluid in the cell. A unit value of F, for example, would equate to a cell full of fluid, whereas a zero value would imply that the cell held no fluid. Cells with F values between 0 and 1 must and have a free surface. Although the VOF technique can locate free boundaries nearly as well as a distribution of marker particles, and with a minimum of stored information, the method is worthless unless an algorithm can be devised for accurately computing the evolution of the F field. The time dependence of F is governed by the equation,

$$\frac{\partial F}{\partial t} + u\frac{\partial F}{\partial x} + v\frac{\partial F}{\partial y} = 0$$

This equation, which is the partial differential equation analogue of marker particles, states that F flows with the above equation reduces to the assumption that F remains constant in each cell in a Lagrangian mesh. In this scenario, F is only used to identify cells that contain fluid.

3.10. Wall Function

In order to save computational time wall functions are often used along with the k-ε model. The wall functions are based upon the relations known from near wall flows. The near wall region can be divided into two different layers, the viscous sublayer and the log-layer. In direct proximity to the wall viscous effects are more dominant than turbulent effects. The further away from the wall the more prominent are the turbulent effects. The region where viscous effects and turbulent effects are approximately equally important is called the buffer-layer. In the log-layer the following relation is valid

$$u = u_T \left(\frac{1}{k}\ln(y^+) + B\right) \tag{3.14}$$

Where,

$$u_T = \left(\frac{\tau}{\rho}\right)^{1/2} \tag{3.15}$$

From (3.15) the dimensionless wall distance y^+ can be constructed

$$y^+ = \frac{y\rho u_T}{\mu} \tag{3.16}$$

When wall functions are used with the k-ε model the log-layer velocity profile (3.14), is applied to the mesh-node closest to the wall. For wall functions used with the k-ε model y^T values in the range 20-100 is recommended [5].

3.11. Free Surface Modelling

One of the most commonly used free surface model in commercial CFD codes is the volume of fluid (VOF) model. In the VOF model each element is given a volume-fraction. If that particular element is occupied by only water the volume-fraction is 1. Analogously an element occupied by only air has volume-fraction 0. In the interface between the two fluids there will be several elements that has values in the range between 0 and 1. It is common to use the volume-fraction value 0.5 to define the surface. The resolution of the mesh in proximity to the water surface is important since it directly impacts how accurate the water surface is [6].

3.12. Assumptions

Throughout this work the following assumptions have been made;

- The flow is assumed to be incompressible.
- The water surface is only subject to the atmospheric pressure.
- The k-ε model is sufficiently accurate to describe the turbulent flow properties.
- No form of temperature differences or temperature driven flow occurs.
- The flow at the inlet is entirely uniform.

3.13. Geometry

The geometry used is a channel with rough walls. The length of the channel is 400 cm and the height is 50 cm.

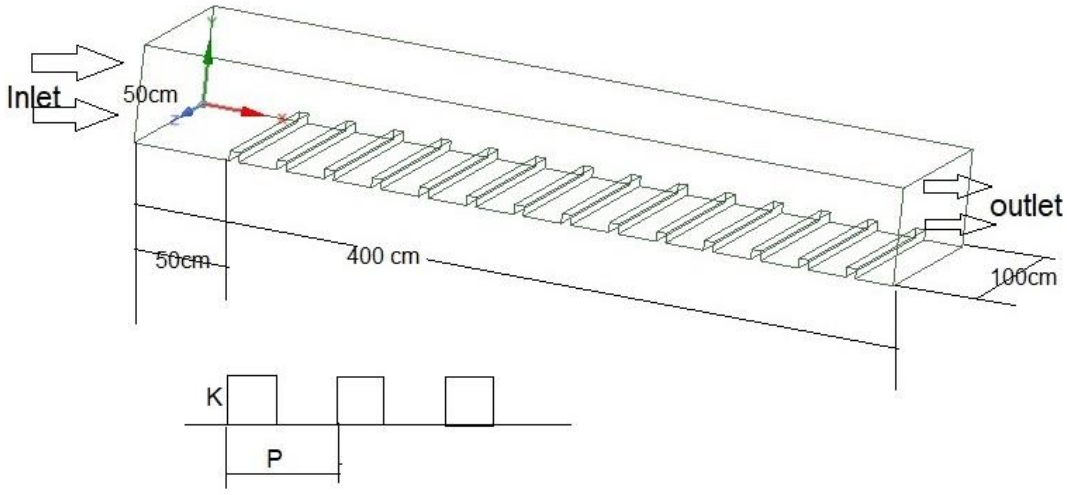

P= pitch K=Rib height= 5cm

(a)k-type roughness (p/k=9) (b)Intermediate roughness (p/k=5)

(c) d-type roughness (p/k=3)

Fig. 3.1: Schematic diagram of the water channel with the transverse square Ribs mounted on the bottom surface

3.14. Boundary Condition

The following boundary conditions are chosen in ANSYS FLUENT.

- The inlet is set as the 'inlet' condition with a turbulent intensity of 5%
- The outlet is set as the 'opening' condition with a zero-gradient volume-fraction condition and a relative pressure set

  $P_{rel} = \rho_{water} y g$, where **g** is the gravity and **y** vary linearly from 0 to the water surface height.
- The rough-walls are set to the 'no-slip wall' condition.

3.15. Meshing

Mesh creation is one of the biggest reasons engineers have a hard time setting up a computational fluid dynamics (CFD) simulation. A rectangular block-structured grid with higher resolution over the recirculation region is the general meshing strategy. In order to fully solve the boundary layer to determine the position of reattachment and separation, the values of Y-plus near the steps are kept near 1. An enhanced wall treatment is used, which allows the solution close to the walls to be computed explicitly. A finer grid is applied to the region where the flow behaviour is expected to be more complex, such as the recirculation regions.

Fig. 3.2(a): Meshing of whole system

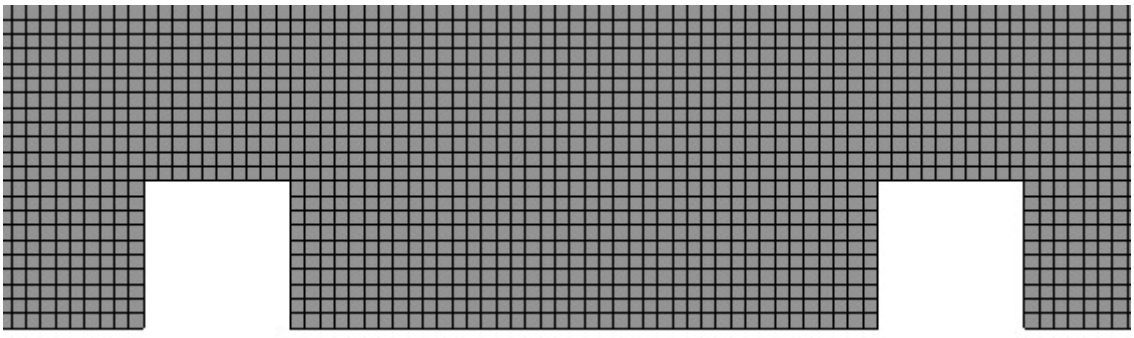

Fig. 3.2(b): Magnified view of mesh:

Nodes = 79731, Elements= 78700

3.16. Named selection

Named selections are essential parameters in ANSYS (Numerical simulation). You can define your named selections on geometry (Faces, Node, and fluid domain), and use them at further boundary condition definitions in ANSYS, Fluent, etc. It is a handy tool for defining boundary conditions in various interfaces of ANSYS. Our geometry named selection is are the following:

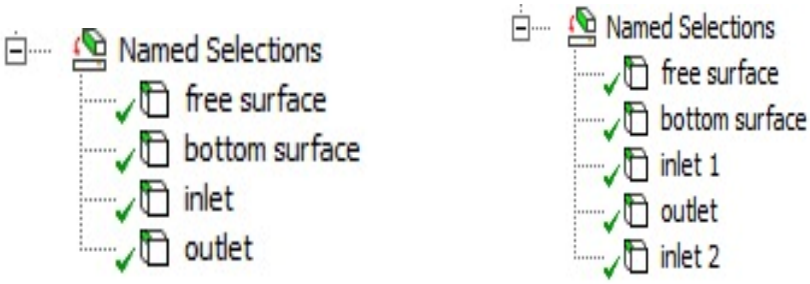

(a) **(b)**

Fig. 3.3, (a) When velocity is given to only water, (b) When velocity is given to both water and air

3.17. Multiphase

There are two different species present in the domain, water and air. The material properties can be seen in table 3.1.

Properties	Water	Air
Phase	Liquid	Gas
Dynamic Viscosity μ [kg/(m·s)]	1×10^{-3}	1.83×10^{-5}
Density ρ [kg/m^3]	998	1.225

Table 3.1: Properties of fluid used in this study

In ANSYS Fluent the multiphase model used is the homogeneous model and the free surface model used is the standard model. Additionally gravitational body forces are present with a downwards gravitational acceleration of 9.81 m/s^2.

Properties	Case I	Case II	Case III
Reynolds number	19,904	39,808	59712
Mean stream velocity	10 cm/sec	20 cm/sec	30 cm/sec
Mean flow depth	20 cm	20 cm	20 cm

Table 3.2: Hydrodynamic conditions for present study

Chapter 4: Study of fluid flow in an open channel over a square rib surface

Case 1: Lower fluid has a constant velocity and upper fluid is at rest

As discussed in previous chapter, three types of roughness pattern are used in this study and these roughness patterns depend upon the value of p/k. This chapter gives us the idea about the velocity contour, nature of streamline, variation of wall shear stress on the transverse face of the rib and velocity distribution within the depth of water above the rib. In case of open channel interaction between water and air happens. So, In this case simulation has been performed by providing inlet velocity to water only.

4.1. Study of the different properties for d-type roughness(p/k=3)

- **Velocity contour for d-type roughness**

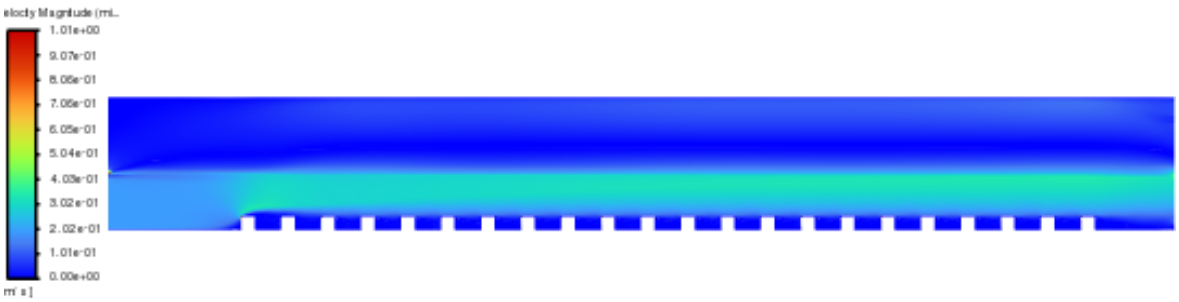

Fig. 4.1: Velocity contour when inlet velocity is 10cm/sec

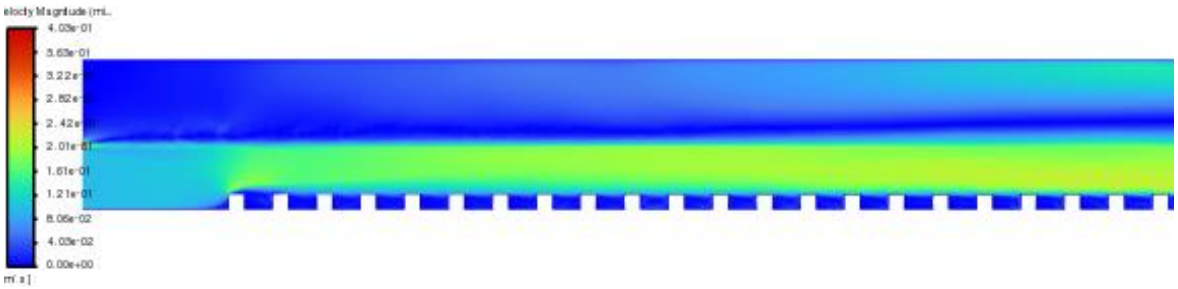

Fig. 4.2: Velocity contour when inlet velocity is 20cm/sec

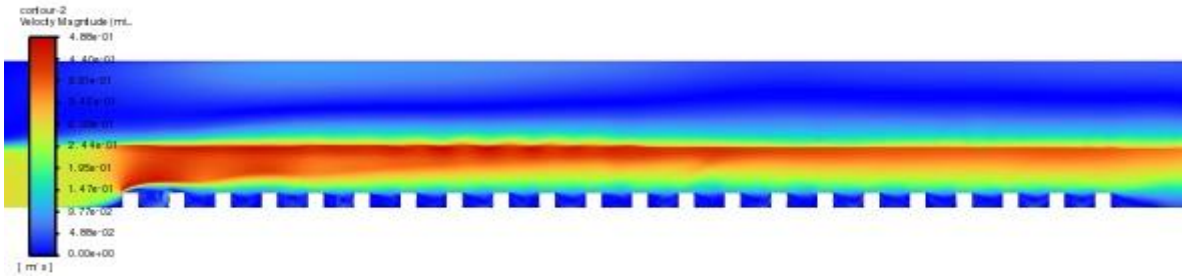

Fig. 4.3: Velocity contour when inlet velocity is 30cm/sec

Figure 4.1, 4.2 and 4.3 represents the velocity profile of the fluid when inlet velocity of water is 10 cm/sec, 20 cm/sec and 30 cm/sec respectively. It is observed that velocity increases abruptly when any disturbance in terms of roughness exists in the path of fluid flowing. A phenomenon is seen from this velocity contour that the velocity of the lower fluid increases suddenly after hitting the first brick and this is happened regularly and repeatedly for all the next ribs. Such type of phenomenon indicates that that there is a chance of energy transformation from pressure energy to velocity energy. Hence, there is a chance of negative pressure gradient which leads the flow separation.

- **Nature of streamline for d-type roughness**

Fig. 4.4: Streamline when inlet velocity is 10 cm/sec

Fig. 4.5: Streamline when inlet velocity is 20 cm/sec

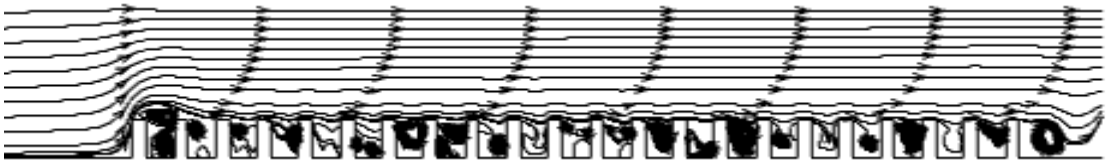

Fig. 4.6: Streamline when inlet velocity is 30 cm/sec

Figure 4.4, 4.5 and 4.6 shows the nature of streamline. The figures of streamline clearly show that the recirculation pattern just after every rib. As the distance between two consecutive rib is very less for d-type roughness; fluid particle after hitting the first rib clearly bypass the second rib when inlet velocity is high (30 cm/sec), but in case of inlet velocity 10 cm/sec fluid particle are hitting again to second rib and so on and so forth. in this case eddy formation is smaller as compare to higher inlet velocity. The formation of eddy is moderate in case of velocity 20 cm/s.

A jumping phenomenon of water also observed while the water hitting the first rib as evident fig. 4.4 to fig 4.6. It is observed that a well-established velocity profile above the

rough part of the channel and flow is smooth and steady. As eddy is formed between every consecutive two square ribs that leads to energy loss.

- **Contour of turbulence kinetic energy**

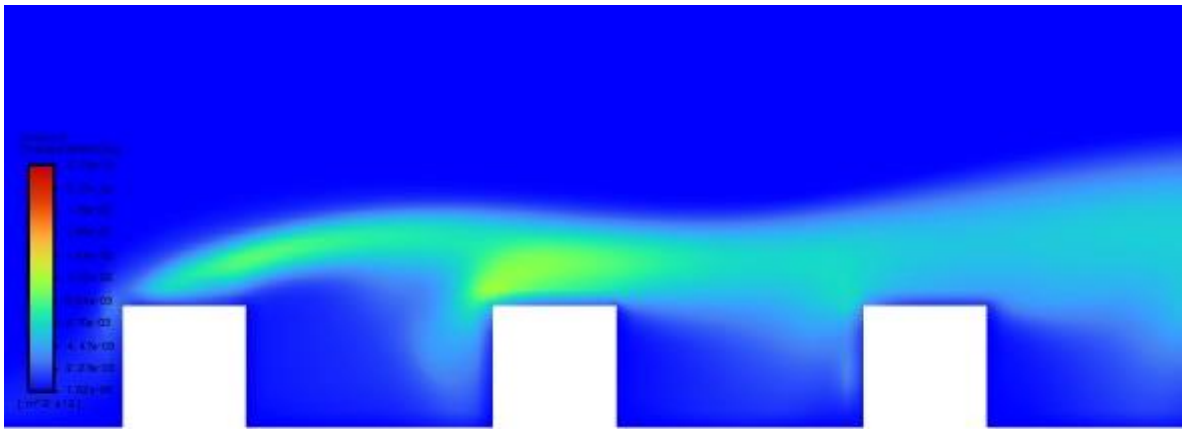

Fig. 4.7: Magnified view of turbulent kinetic energy for d-type roughness (p/k=3) (When inlet velocity is 30 cm/sec)

Turbulence kinetic energy (TKE) is the mean kinetic energy per unit mass associated with eddies in turbulent flow in fluid dynamics. Turbulence kinetic energy is defined physically by measured root-mean-square (RMS) velocity variations. An interesting feature of TKE is seen from the fig 4.7 that the TKE just above the brick is comparatively more than the other parts of the channel under consideration. Turbulence intensity is maximum near the top of the roughness due to the presence of shear layer.

4.2. Study of the different properties for intermediate roughness (p/k=5)

- **Velocity contour for intermediate type of roughness**

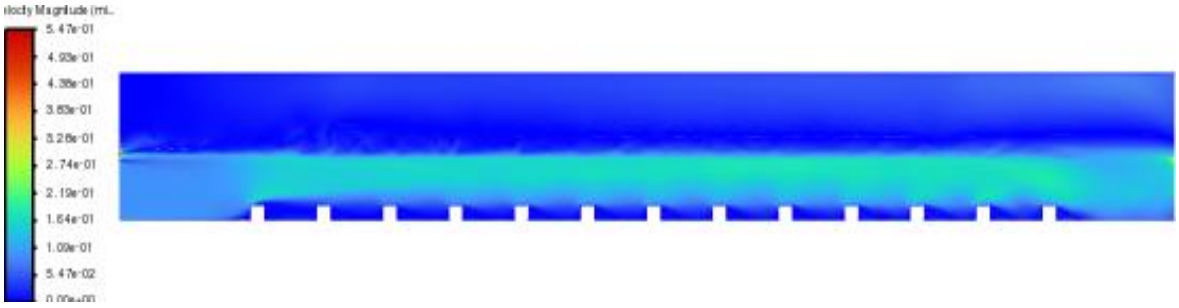

Fig. 4.8: Velocity contour when inlet velocity is 10 cm/sec

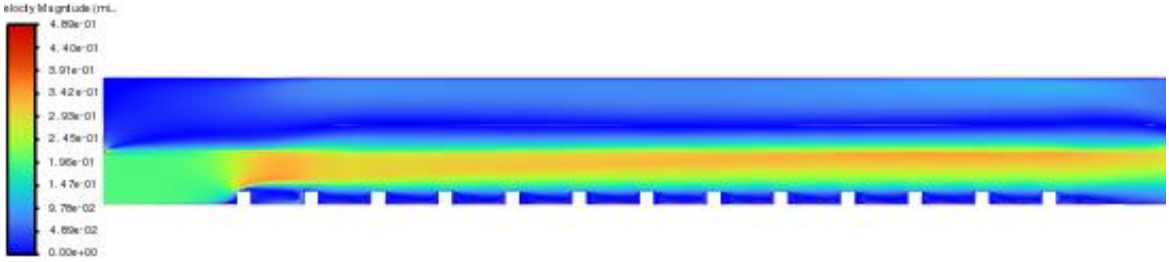

Fig. 4.9: Velocity contour when inlet velocity is 20 cm/sec

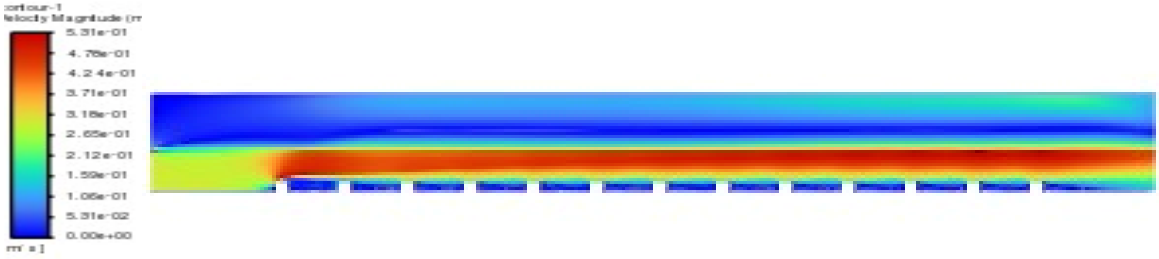

Fig. 4.10: Velocity contour when inlet velocity is 30 cm/sec

A similar study has been carried out for intermediate roughness (p/k=5), and Figure 4.8, 4.9 and 4.10 represents the velocity profile of the flowing fluid for the velocity 10 cm/sec, 20 cm/sec and 30 cm/sec respectively, and almost similar pattern of the velocity contour have been developed. In this case, it is found that the increment of velocity also is seen on second brick or rib. Hence, an impact of intermediate roughness is established through this study.

- **Nature of streamline**

Fig. 4.11: Velocity streamline when inlet velocity is 10 cm/sec

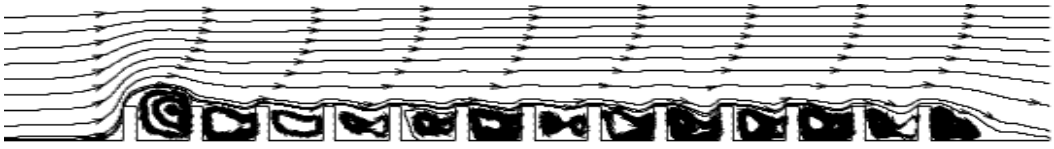

Fig. 4.12: Velocity streamline when inlet velocity is 20 cm/sec

Fig. 4.13: Velocity streamline when inlet velocity is 30 cm/sec

Figure 4.11, 4.12 and 4.13 shows the nature of streamline. Similar to previous case it clearly shows the recirculation pattern just after every rib. As the distance between two rib is more as compare to d-type roughness so fluid particle after hitting the first rib tend to bypass the second rib when inlet velocity is high (30 cm/sec) and when the inlet velocity of fluid particle decreases then there are chance of hitting to second rib and this can be clearly seen from nature of the stream line figure. It is very prominent for the low inlet velocity as evident fig.4.11.

4.3. Study of the different properties for k-type roughness(p/k=9)

- **Velocity contour for k-type roughness**

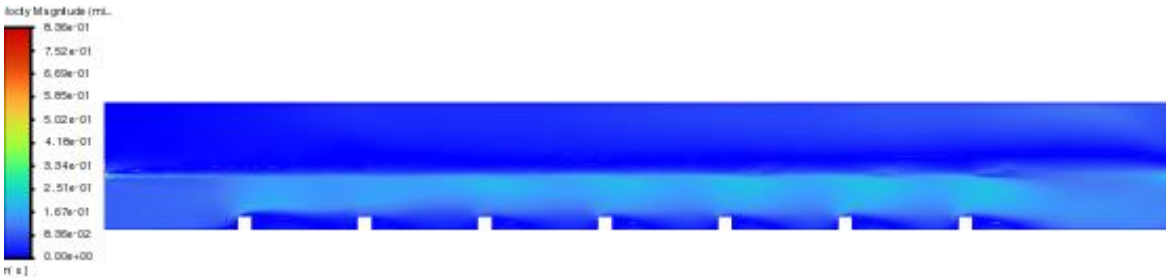

Fig. 4.14: Velocity contour when inlet velocity is 10 cm/sec

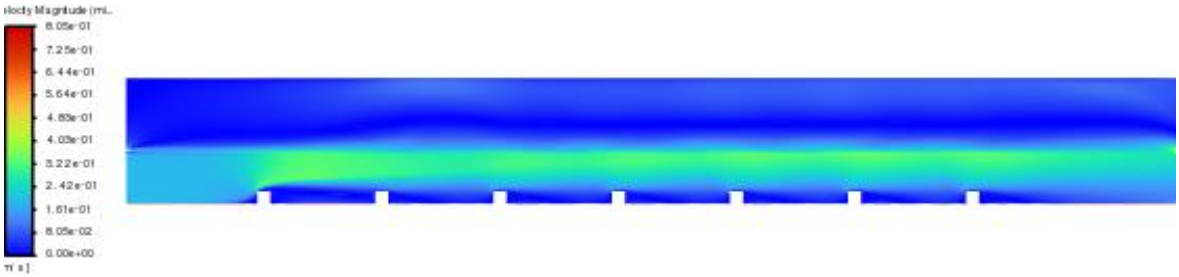

Fig. 4.15: Velocity contour when inlet velocity is 20 cm/sec

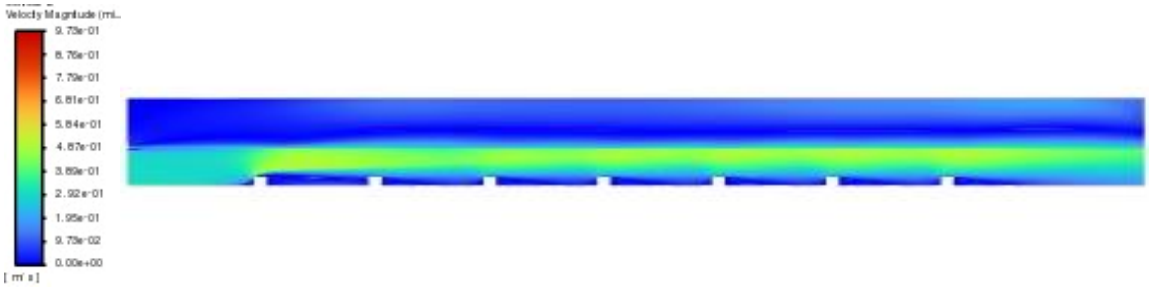

Fig.4.16: Velocity contour when inlet velocity is 30 cm/sec

It is observed from the velocity contour of all three types of roughness that the velocity fluctuation is more for k-type of roughness (p/k=9) as evident figs. 4.14, 4.15, 4.16. This is so because, this type of roughness creates more space between two consecutive ribs so that

water can be filled in smoothly and again hit the brick in previous manner, but for d-type and intermediate type of roughness, the space between two consecutive brick is less resulting in insignificant fluctuation of water. The back flow or eddy formation of the water in the intermediate space of two consecutive ribs is very significant in this case which cause of the huge energy loss of the flowing fluid in the k-type roughness and this energy loss creates the velocity fluctuation throughout the channel.

- **Nature of streamline**

Fig. 4.17: Velocity streamline when inlet velocity is 10 cm/sec

Fig. 4.18: Velocity streamline when inlet velocity is 20 cm/sec

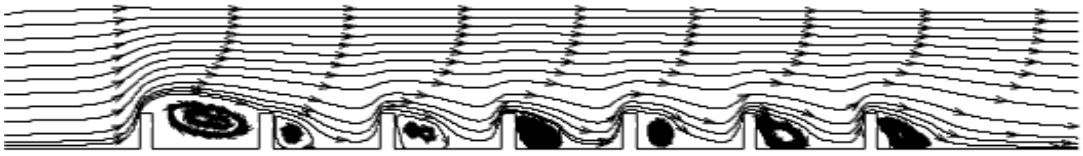

Fig. 4.19: Velocity streamline when inlet velocity is 30 cm/sec

From the streamline as shown in figs. 4.17, 4.18 and 4.19 for all three types of roughness namely d-type, intermediate type and k-type roughness it is visible that there is a creation of recirculation zone, and the extent of this recirculation zone is depending on the space between two consecutive rib or the value of inlet velocity. As from above figure of streamline for all type of roughness it is established that the when distance between two rib is more, then the more stream line hit the all the ribs. From above streamline, it is clear that the pattern of eddy formation is nearly same when inlet velocity is less or space between two ribs is more, and because of this recirculation zone there is some irregularity in case of wall shear stress which can be seen in the next.

4.4. Comparison for the wall shear stress and velocity distribution for different types of roughness and different inlet velocity

4.4.1. Variation of Wall shear stress on the transverse face of rib for d-type roughness (p/k=3)

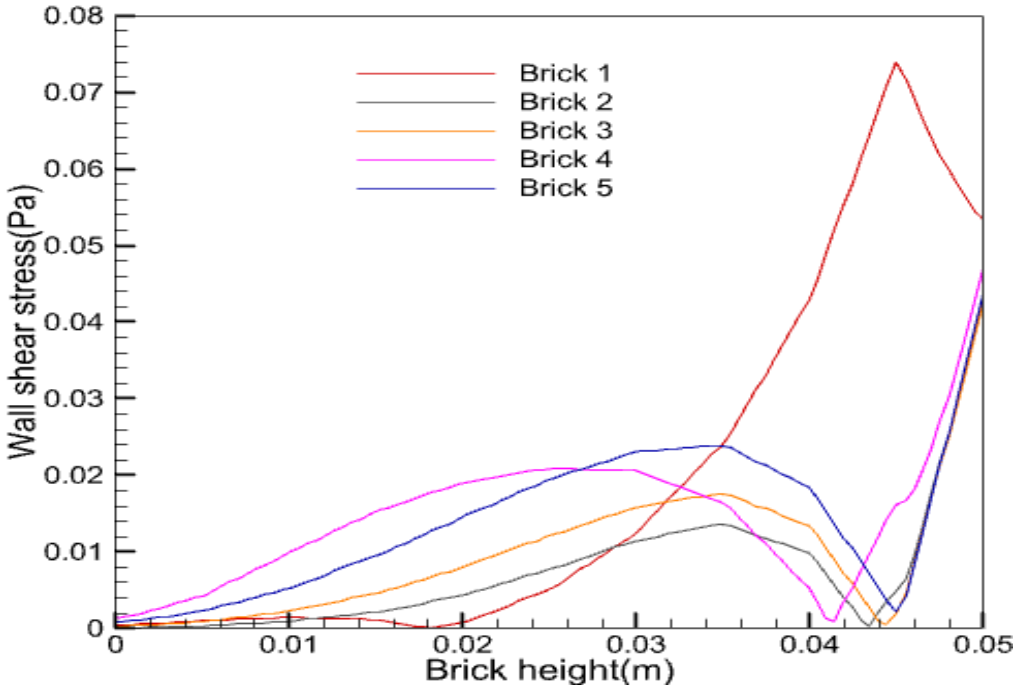

Fig. 4.20: Wall shear stress distribution when inlet velocity is 10 cm/sec

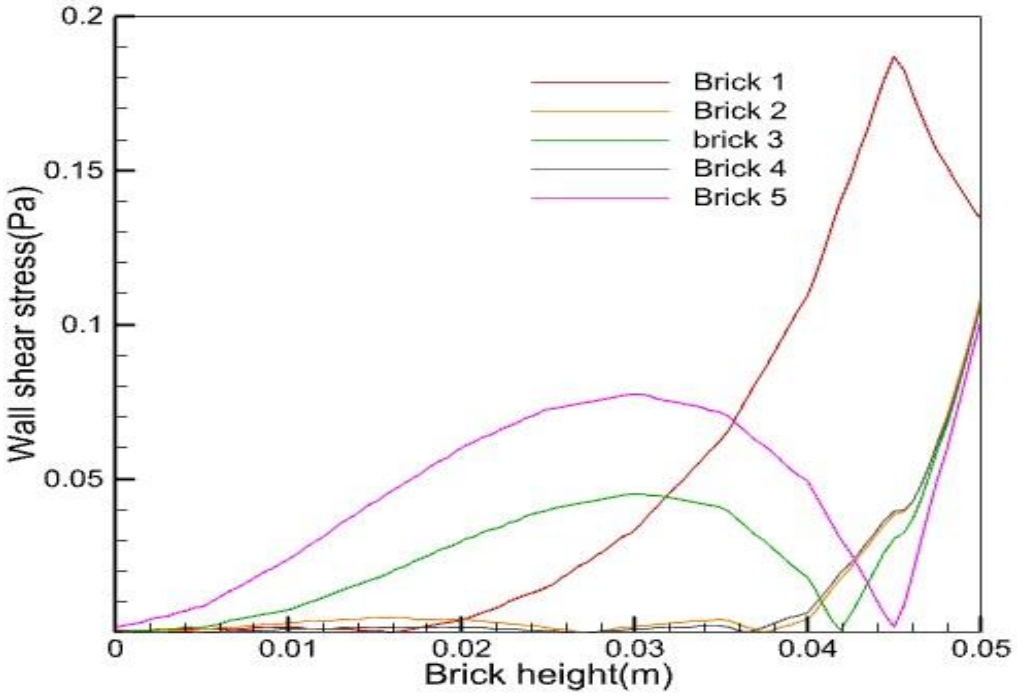

Fig. 4.21: Wall shear stress distribution when inlet velocity is 20 cm/sec

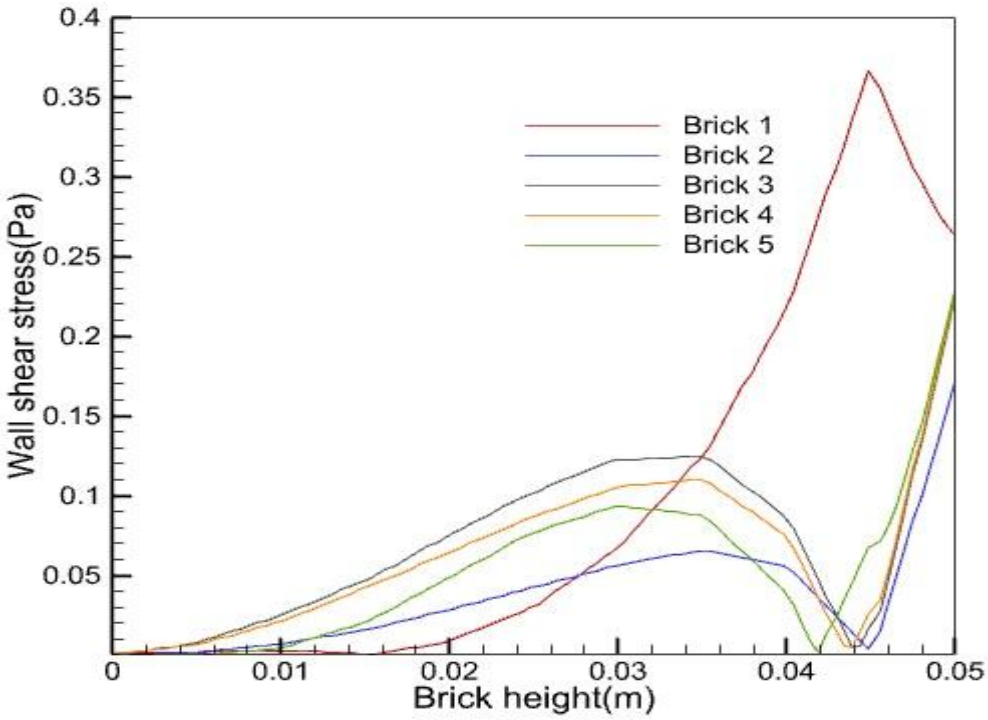

Fig.4.22: Wall shear stress distribution when inlet velocity is 30 cm/sec

Figure 4.20, 4.21 and 4.22 represents the graphical presentation of wall shear stress on the transverse wall of rib for d-type roughness. From the above presentation, it is clear that wall shear stress on the first rib is completely different from all other rib as fluid particle are not hitting all the rib in same manner. From above graph, it can be analysed that for d-type of roughness wall shear stress first increases and then becomes zero at just below the corner point of rib and again starts increasing. Figure 4.21 shows that wall shear stress for brick 2 is almost zero and this is because of after hitting on first brick fluid particle bypasses the second rib so no impact is occurring on the second rib, similarly the same phenomena is observed in case of fourth brick.

4.4.2. Variation of wall shear stress on the transverse face of rib for intermediate roughness(p/k=5)

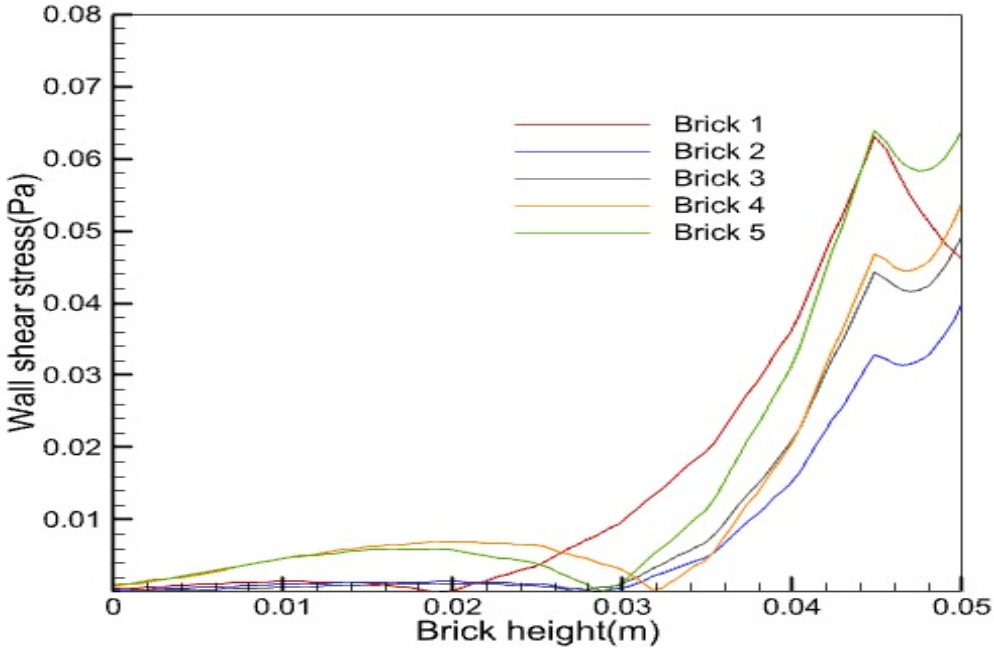

Fig. 4.23: Wall shear stress distribution when inlet velocity is 10 cm/sec

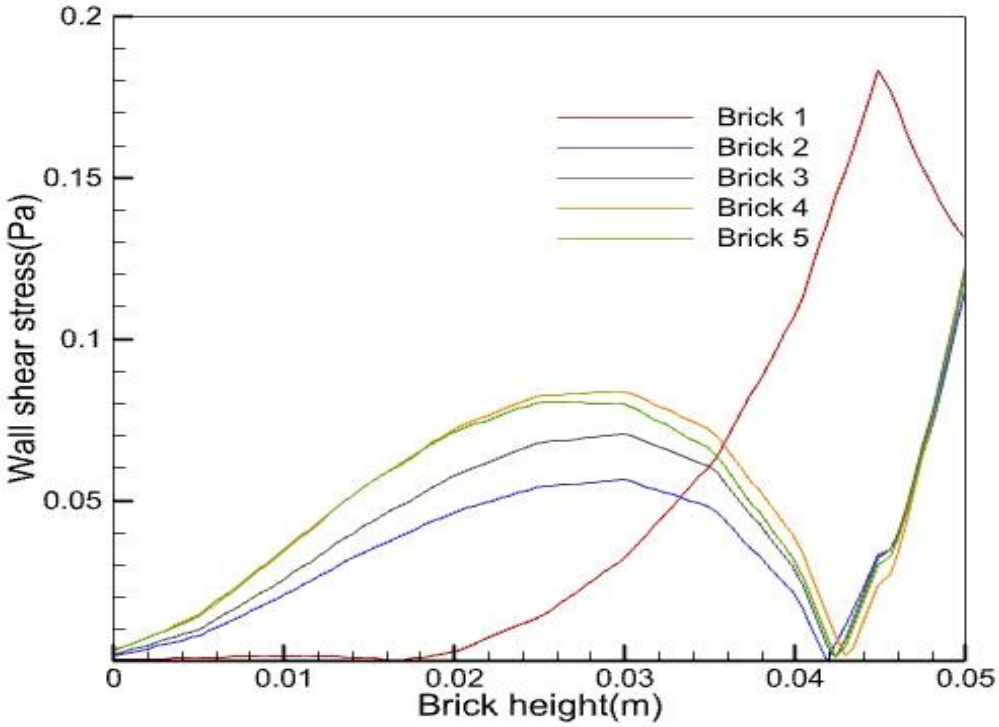

Fig. 4.24: Wall shear stress distribution when inlet velocity is 20 cm/sec

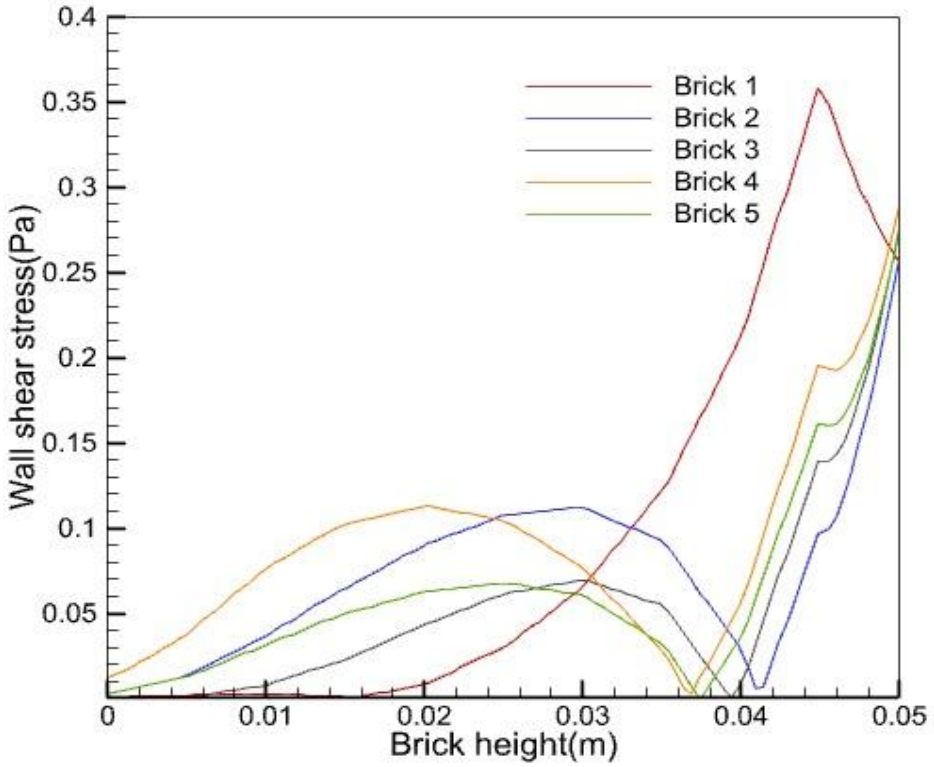

Fig. 4.25: Wall shear stress distribution when inlet velocity is 30 cm/sec

Figure 4.23, 4.24 and 4.25 represents the plot of wall shear stress on the transverse wall of rib for intermediate type of roughness. From the above figs, it is clear that wall shear stress on the first rib is completely different from all other rib as fluid particle are not hitting all the rib in same manner. It observed that for intermediate type of roughness variation of wall shear stress is slightly different from d-type roughness as in this case wall shear stress first increases and then becomes zero at just below the corner point of rib and again starts increasing but in the figure 4.23 when velocity is less (10 cm/sec), variation of wall shear stress at the corner is different because of low velocity gradient.

4.4.3. Variation of wall shear stress on the transverse face of rib for k-type roughness

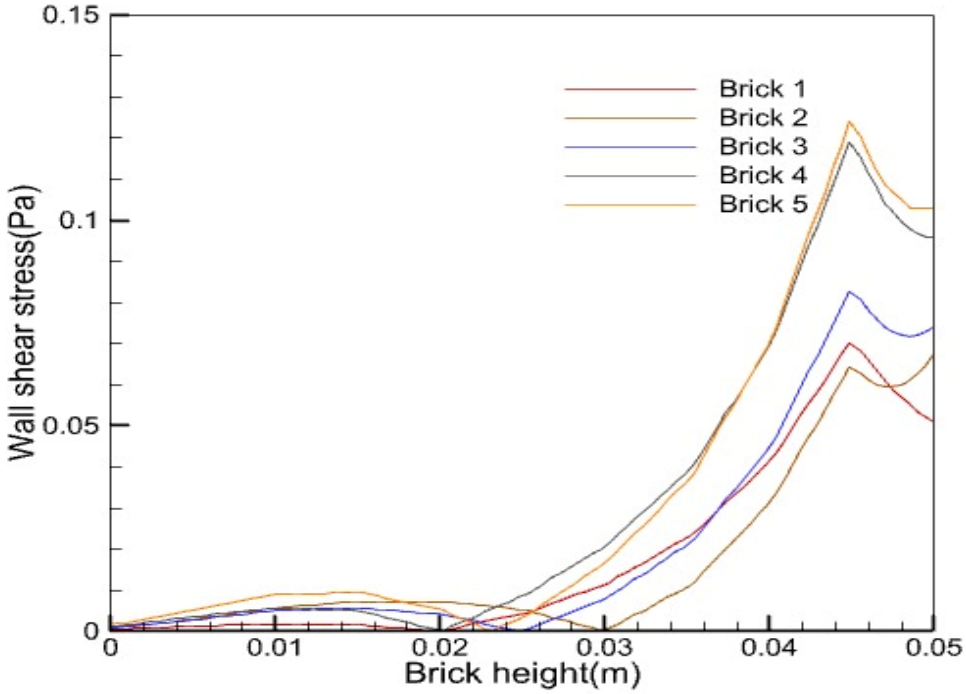

Fig. 4.26: Wall shear stress distribution when inlet velocity is 10 cm/sec

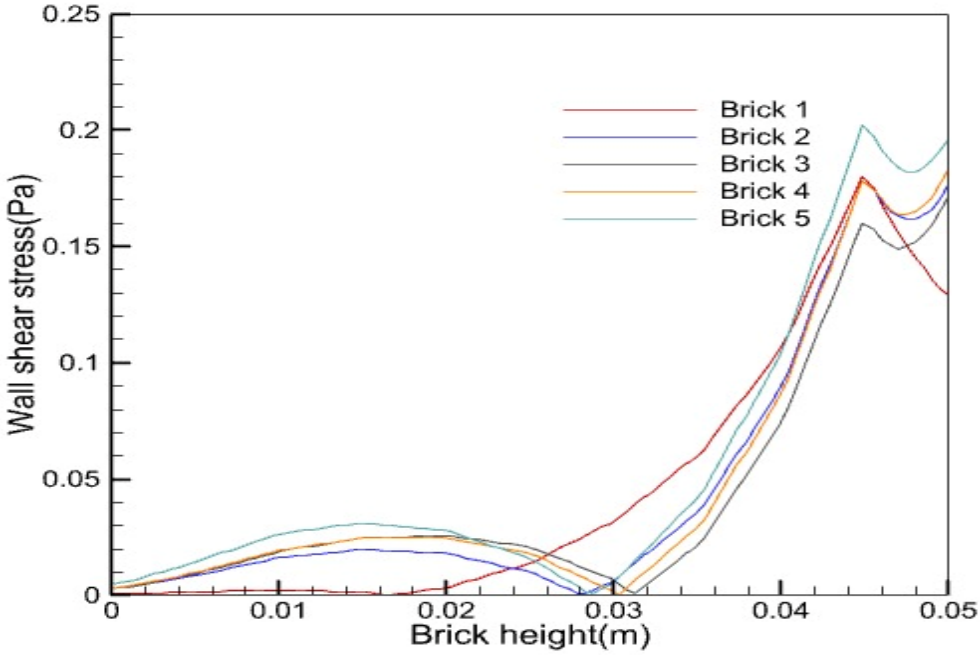

Fig. 4.27: Wall shear stress distribution when inlet velocity is 20 cm/sec

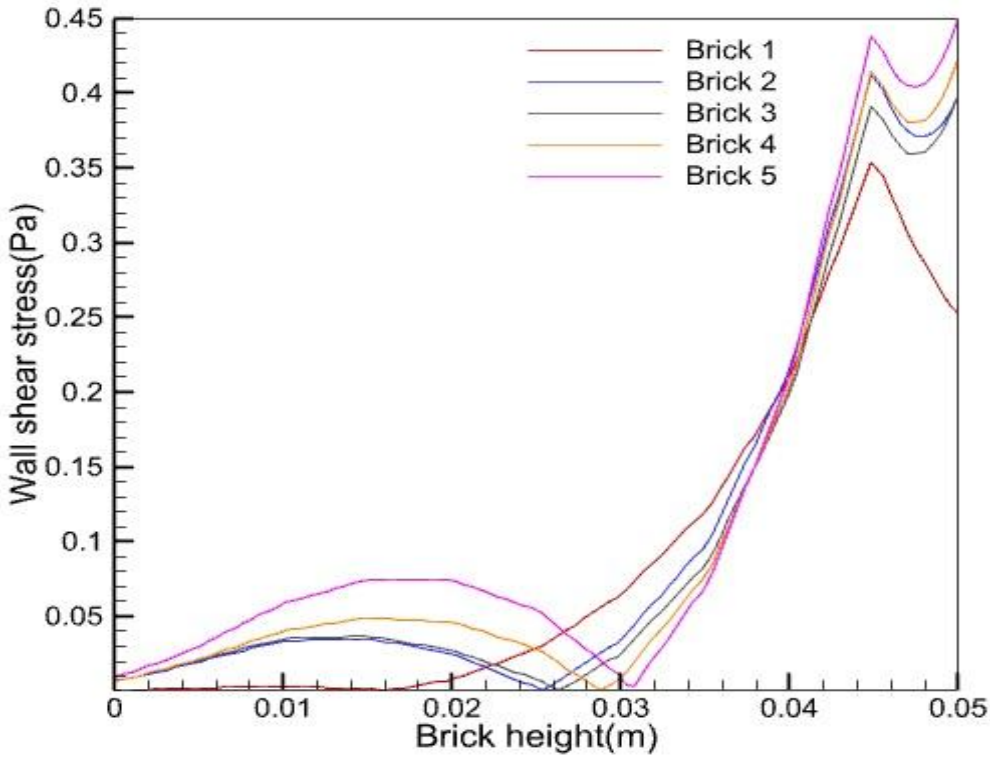

Fig.4.28: Wall shear stress distribution when inlet velocity is 30 cm/sec

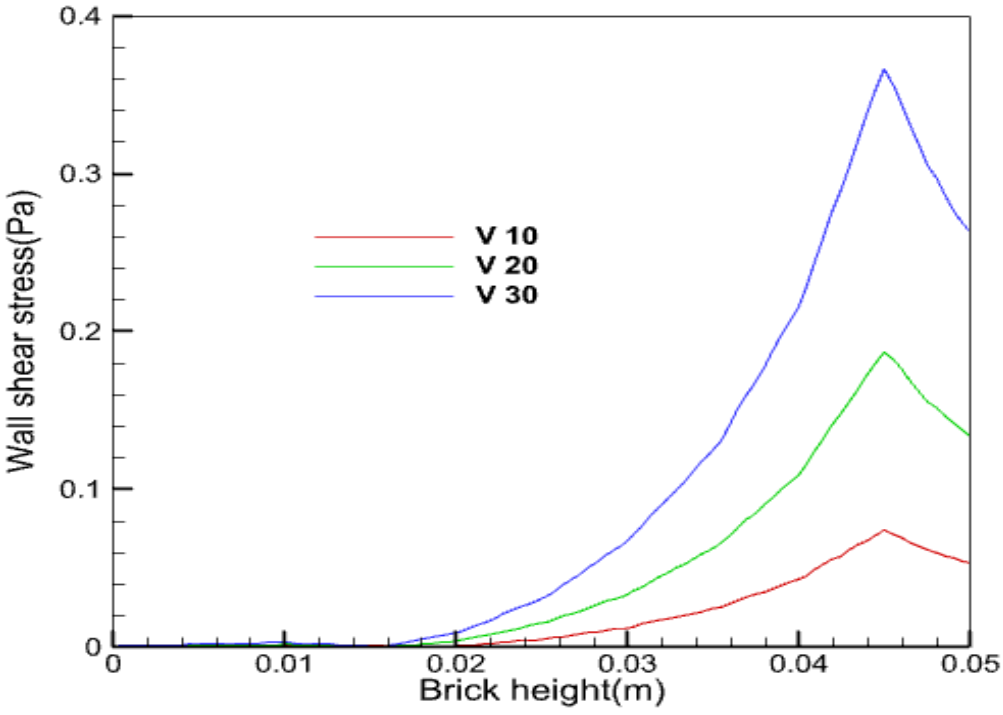

Fig. 4.29: Variation of wall shear stress on first rib for velocity 10, 20 and 30 cm/sec

Figure 4.26, 4.27 and 4.28 represents the pattern of wall shear stress on the transverse wall of rib for k-type of roughness, and figure 4.29 represents the variation of wall shear stress on the first brick for different inlet velocity.

From figs it is observed that the variation of wall shear stress for k-type roughness is completely different from d-type roughness as the space between two consecutive rib is more in this case. Nature of wall shear stress is approximately same for low inlet velocity and high p/k value. While finding the effective wall shear stress there are several points on which this simple analysis could be criticized. First, the streamlines close to the crests of the elements are most probably wavy in nature [1]. So, the irregularities in wall shear stress on the transverse face of brick 1 and brick 2 and so on have been representing in the figures. As near the corner of brick surface recirculation zone is taking place and it is clearly seen from the streamline figure, which leads the large velocity gradient near the wall.

4.4.4. Velocity fluctuation within the depth of water above the rib for d-type roughness

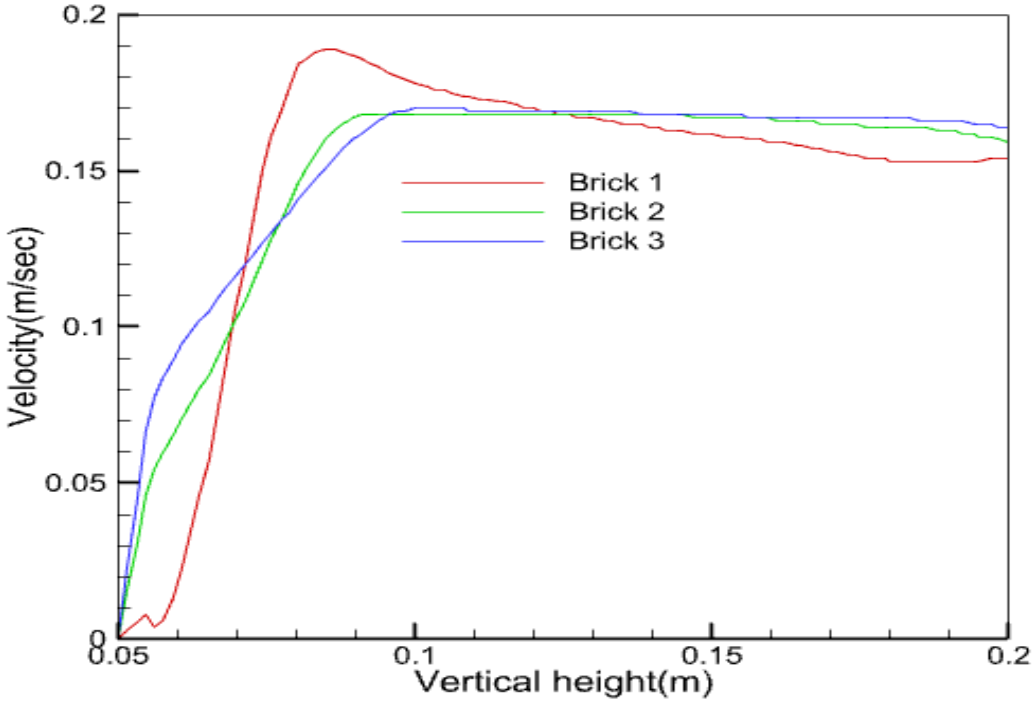

Fig. 4.30: Velocity fluctuation when inlet velocity is 10 cm/sec

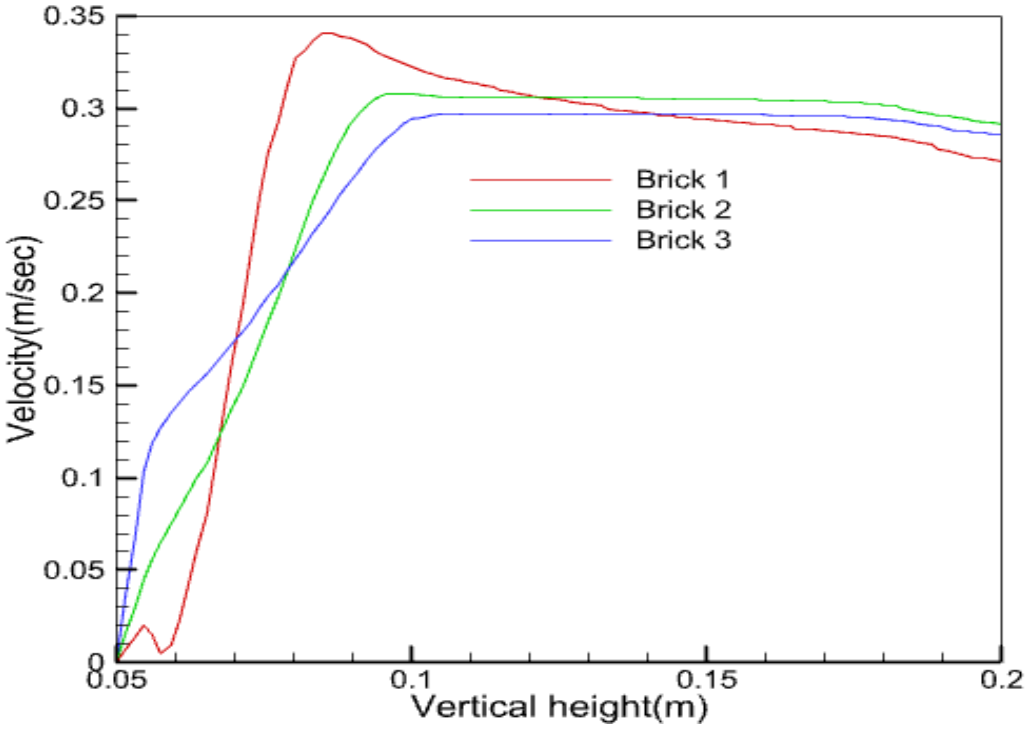

Fig. 4.31: Velocity fluctuation when inlet velocity is 20 cm/sec

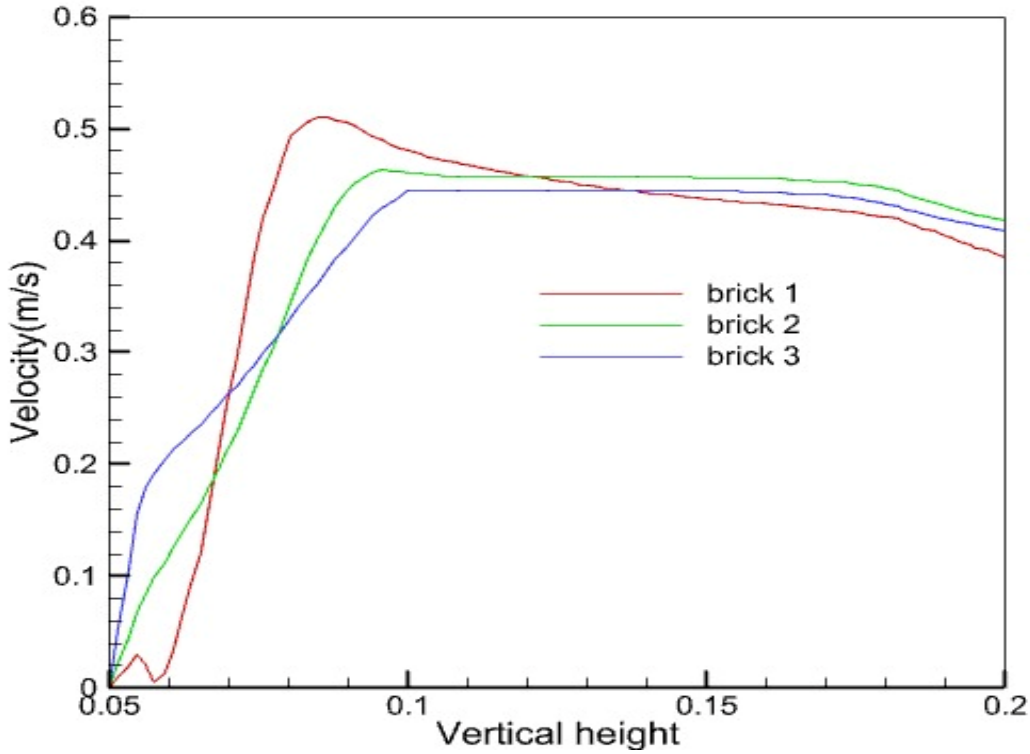

Fig.4.32: Velocity fluctuation when inlet velocity is 30 cm/sec

4.4.5. Velocity fluctuation within the depth of water above the rib for intermediate roughness

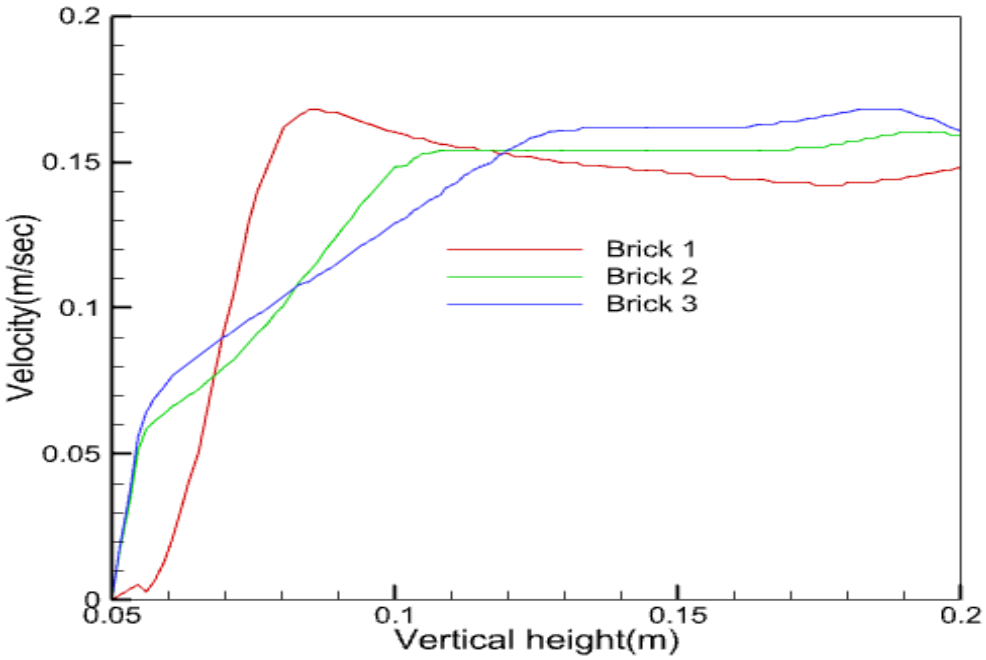

Fig. 4.33: Velocity fluctuation when inlet velocity is 10 cm/sec

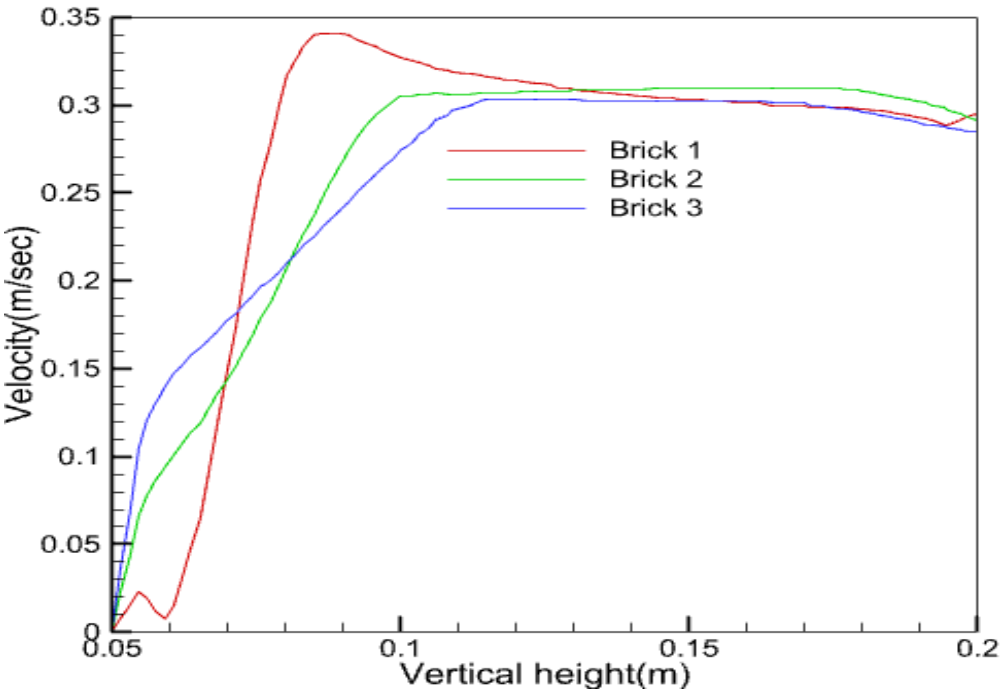

Fig. 4.34: Velocity fluctuation when inlet velocity is 20 cm/sec

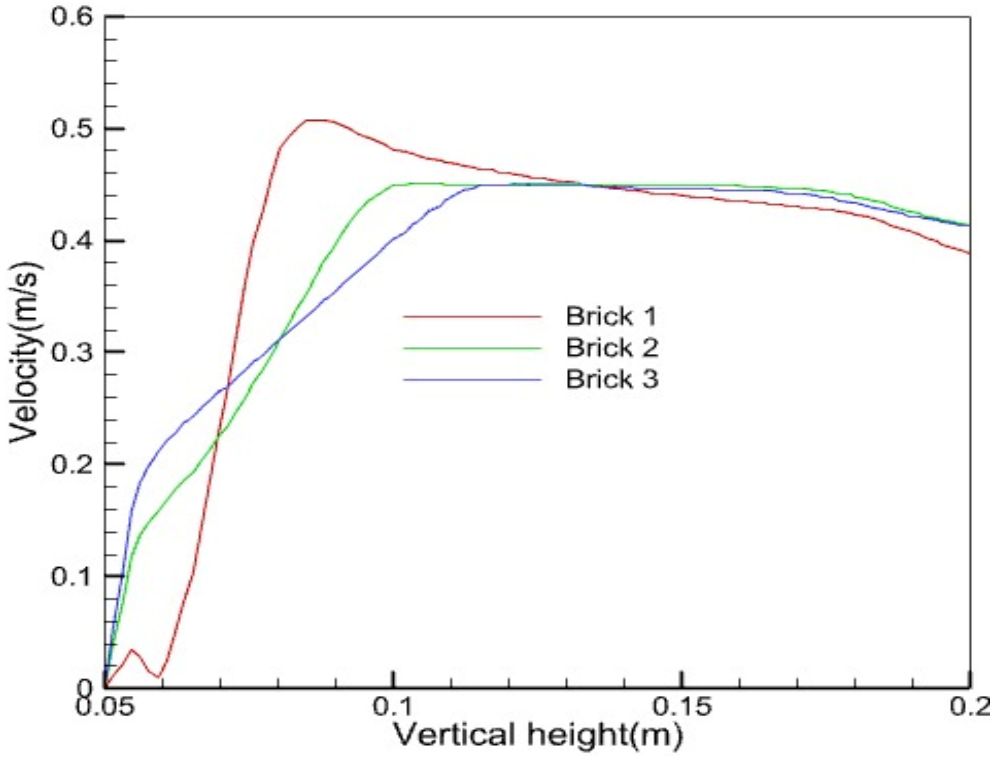

Fig. 4.35: Velocity fluctuation when inlet velocity is 30 cm/sec

4.4.6. Velocity fluctuation within the depth of water above the rib for k-type roughness

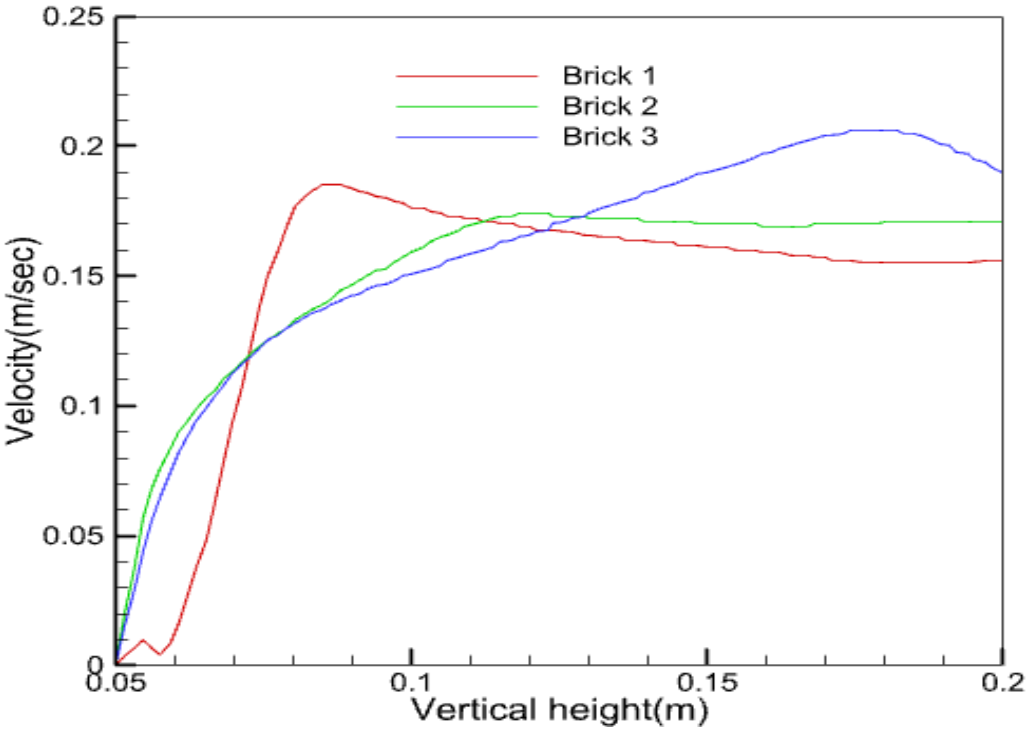

Fig. 4.36: Velocity fluctuation when inlet velocity is 10 cm/sec

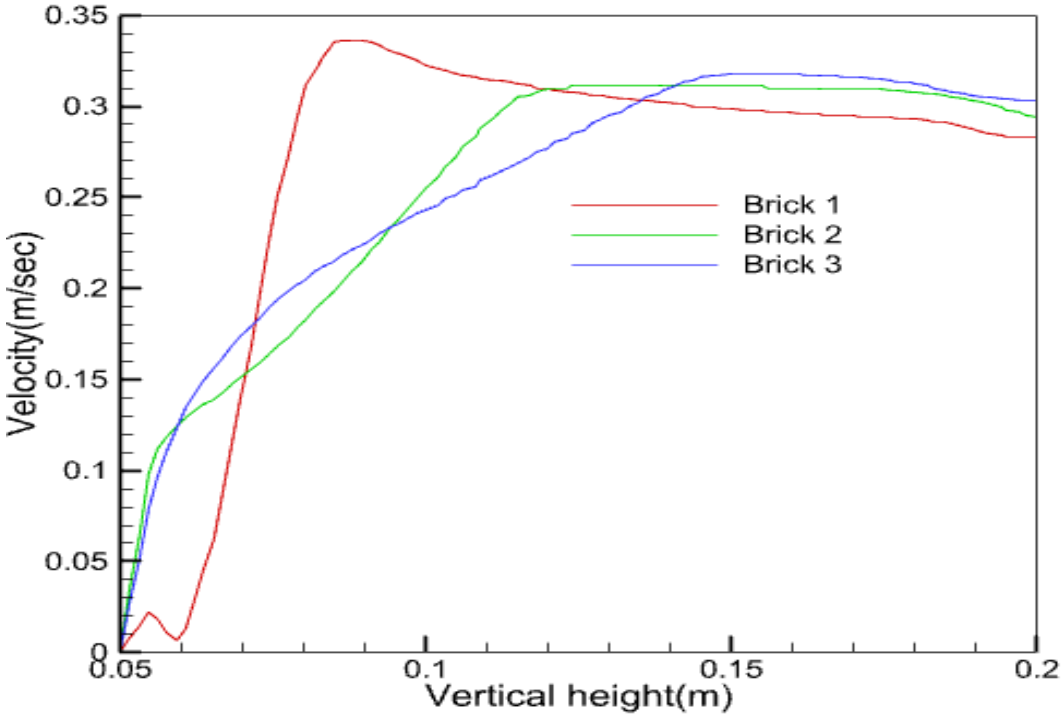

Fig. 4.37: Velocity fluctuation when inlet velocity is 20 cm/sec

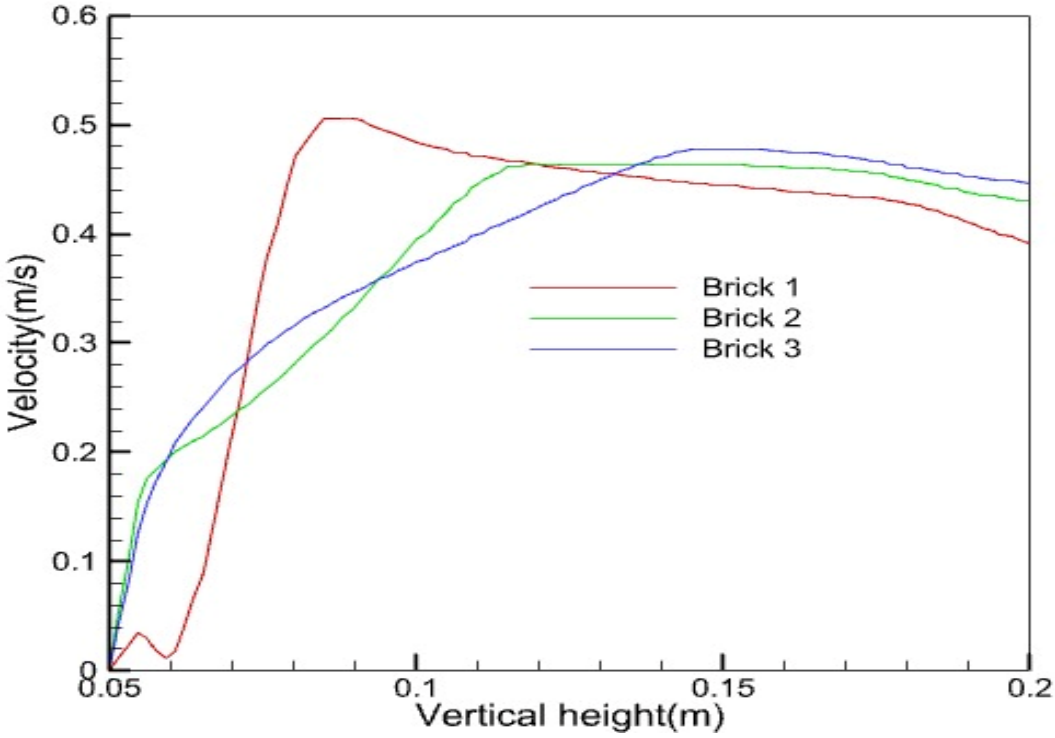

Fig. 4.38: Velocity fluctuation when inlet velocity is 30 cm/sec

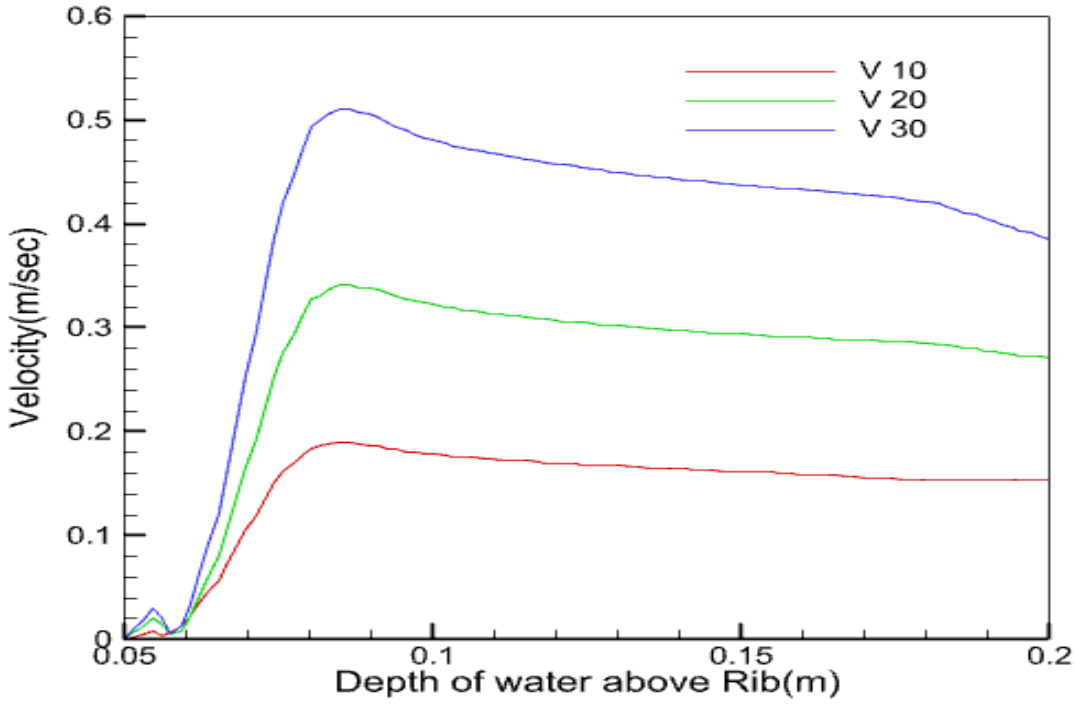

Fig. 4.39: Velocity fluctuation above the first rib

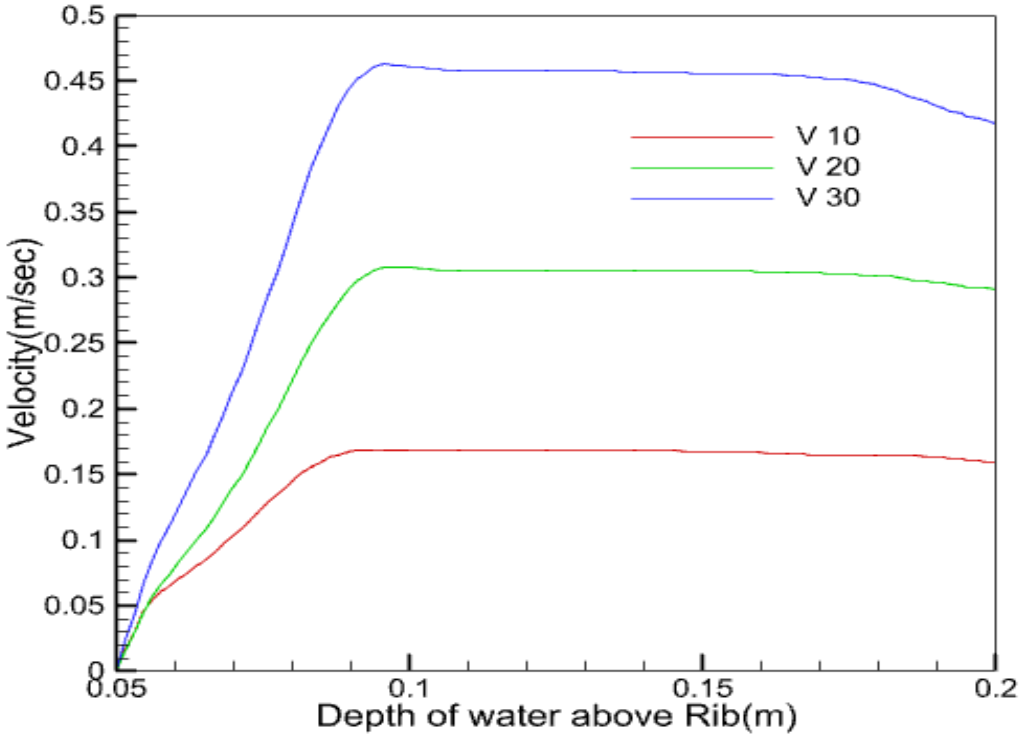

Fig. 4.40: Velocity fluctuation above the second rib for d-type roughness

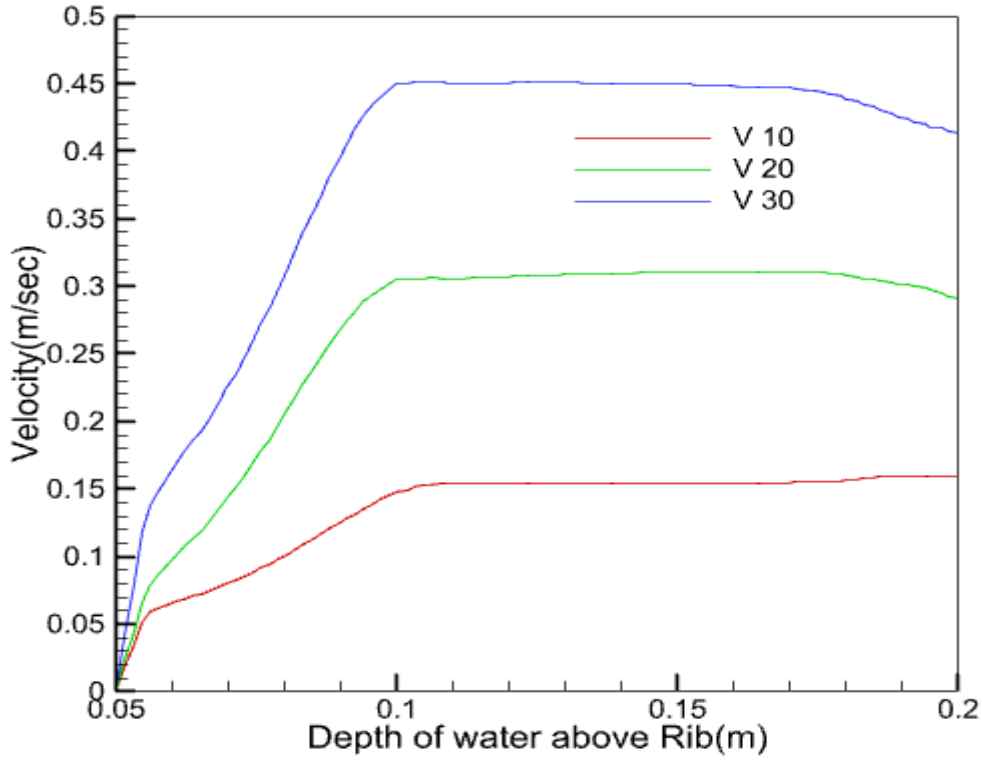

Fig. 4.41: Velocity fluctuation above the second rib for intermediate roughness

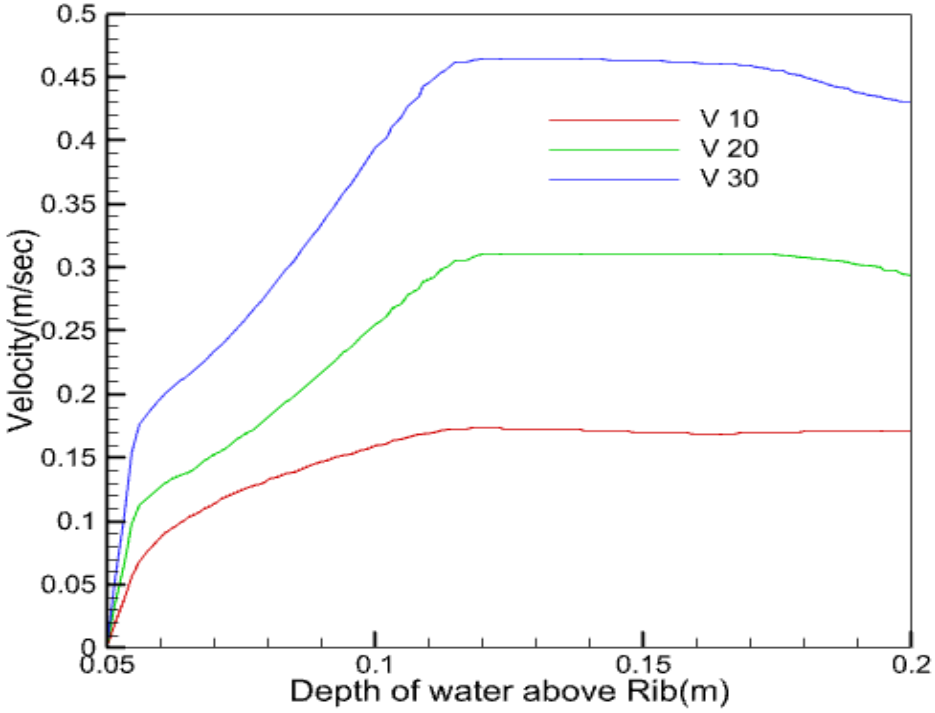

Fig. 4.42: Velocity fluctuation above the second rib for k-type roughness

Figure 4.30, 4.31 and 4.32 represents the velocity fluctuation for d-type roughness and figure 4.33, 4.34 and 4.35 represents the velocity fluctuation for intermediate roughness and figure 4.36, 4.37 and 4.38 represents the velocity fluctuation for k-type roughness within the depth of water taken above the rib for inlet velocity 10 cm/sec, 20 cm/sec and 30 cm/sec respectively.

In this study, first three consecutive bricks are considered to identify the nature of the velocity fluctuation for d-type roughness, intermediate type roughness and k-type roughness. It is observed that the nature of the velocity fluctuation is more after the first rib. Initially velocity is zero above the rib because of no slip condition. Therefore, from this analysis it is clear that the increment of velocity on the second and third rib is more for intermediate type of roughness and k-type roughness as compare to d-type roughness.

It is visualised that after hitting the brick velocity increases and then the increment of velocity is depending upon the type of roughness. As in d-type of roughness fluid particle after hitting the first rib bypasses the second rib and it will not hit the second rib in proper manner so no increment of velocity is seen, but for intermediate type and k-type roughness fluid particle hits the second and third rib also in previous manner so in this case increment in velocity can be seen.

Roughness pattern	**Position**	**Maximum velocity (cm/sec)**		
		10 cm/sec	**20 cm/sec**	**30 cm/sec**
d-type	Rib 1	19.27	34.56	50.89
	Rib 2	15.67	30.58	48.79
	Rib 3	16.85	28.57	43.85
Intermediate type	Rib 1	19.29	34.87	50.89
	Rib 2	15.68	30.68	44.89
	Rib 3	16.28	29.57	44.76
k-type	Rib 1	19.67	34.67	50.37
	Rib 2	18.52	31.27	46.27
	Rib 3	21.57	32.57	48.29

Table 4.1: Maximum velocity attained just after hitting the rib

Reynolds number ($R_e = \frac{\rho v d}{\mu}$) is directly proportion to velocity, as other parameters are remains constant for this study, hence the nature of variation of the Reynolds number is same as velocity variation within the depth of water above the rib.

Figure 4.30, 4.33 and 4.36 shows the effects of roughness pattern (space between the two consecutive ribs) in the bottom surface of an open channel. It is observed that the fluctuation in velocity is more for k-type of roughness as compare to d-type roughness.

Chapter 5: Study of fluid flow in an open channel over a square rib surface

Case 2: Both the Lower fluid and upper fluid have a constant velocity

In this chapter, different types of contours mainly velocity, stream line and turbulent kinetic energy have been discussed for all types of roughness model namely d-type, intermediate type and k-type of roughness based on the p/k value considering the lower fluid and upper fluid both having a constant. In this study, velocity at inlet for both fluid is 30 m/s. The upper fluid is air and the lower one is water. The variation of wall shear stress and velocity fluctuation with vertical depth is also studied.

5.1. Contour for different type of roughness

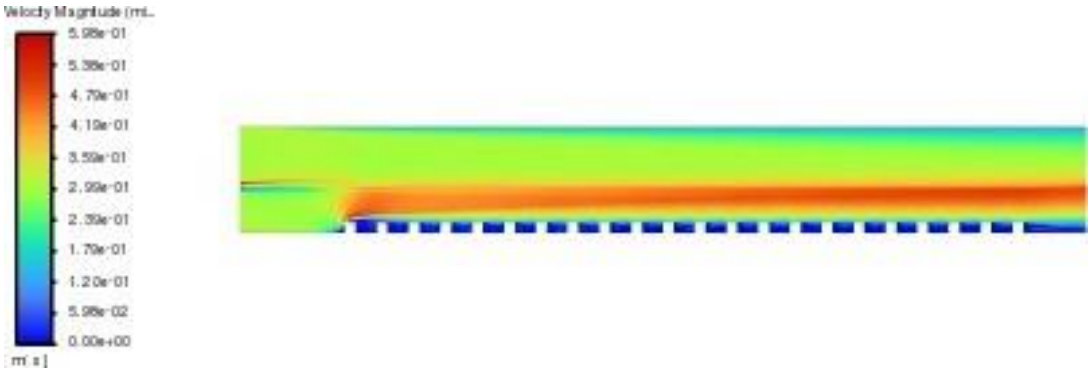

Fig. 5.1: Velocity contour for d-type roughness (p/k=3)

Fig. 5.2: Velocity streamline for d-type roughness (p/k=3)

From the fig.5.1 and 5.2, it is visualized that the velocity fluctuation is almost same as case 1 where the upper fluid is at rest. Velocity of flowing fluid increases abruptly when the fluid faces any disturbance in the path of flow. The same phenomenon is observed as previous case for the velocity of lower fluid. So, it is noticeable that the velocity of the upper layer has no such influence in the lower layer fluid in case of open channel flow.

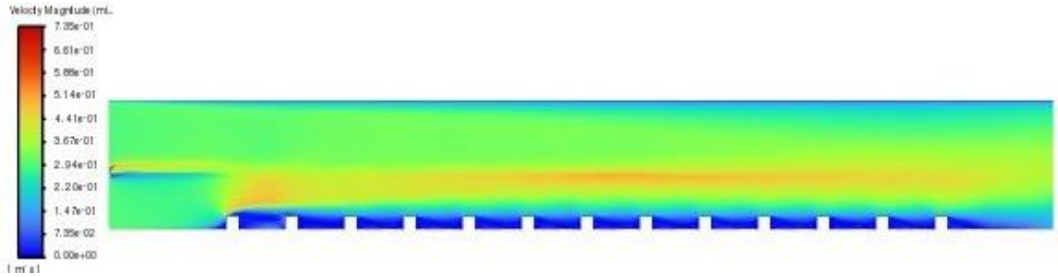

Fig. 5.3: Velocity contour for intermediate type roughness (p/k=5)

Fig. 5.4: Velocity streamline for intermediate-type roughness (p/k=5)

From above contours (Fig.5.3 and 5.4), it is seen that intermediate type of roughness the velocity fluctuation past the rib is more uniform as compare to d-type roughness and the same nature also found in case 1.

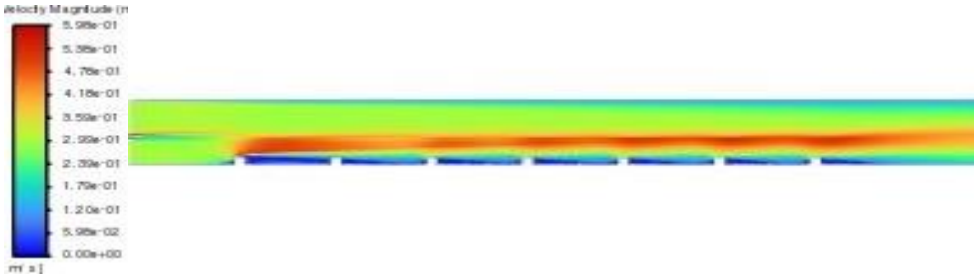

Fig. 5.5: Velocity contour for k-type roughness (p/k=9)

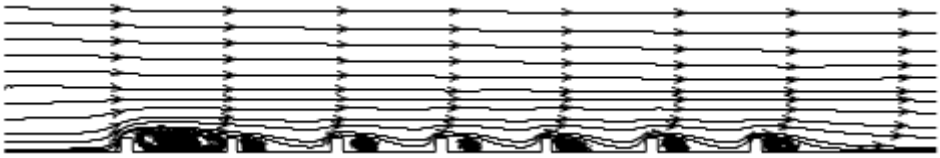

Fig. 5.6: Velocity streamline for k-type roughness (p/k=9)

For k-type of roughness as the gap between the two consecutive ribs is more as shown in fig 5.5 and fig 5.6, so flowing water will hit all the brick in almost same manner. The nature of the streamline is slightly different from the d-type and intermediate type. So the impact of the streamline is more significant in this case.

5.2. Comparison for the wall shear stress and velocity distribution for different types of roughness

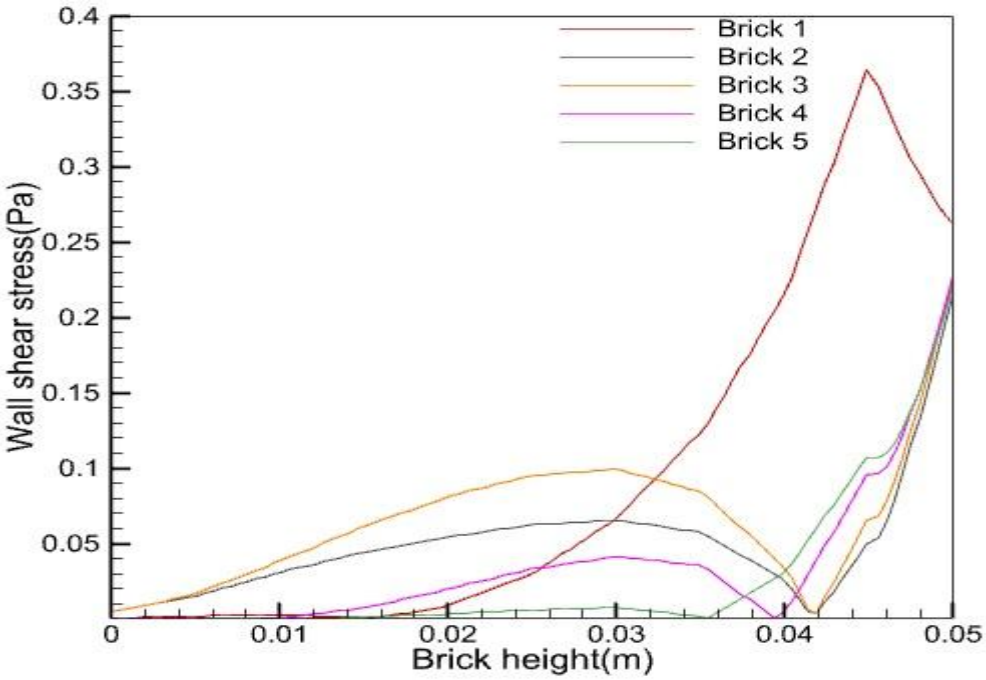

Fig. 5.7: Wall shear stress distribution for d-type roughness (p/k=3)

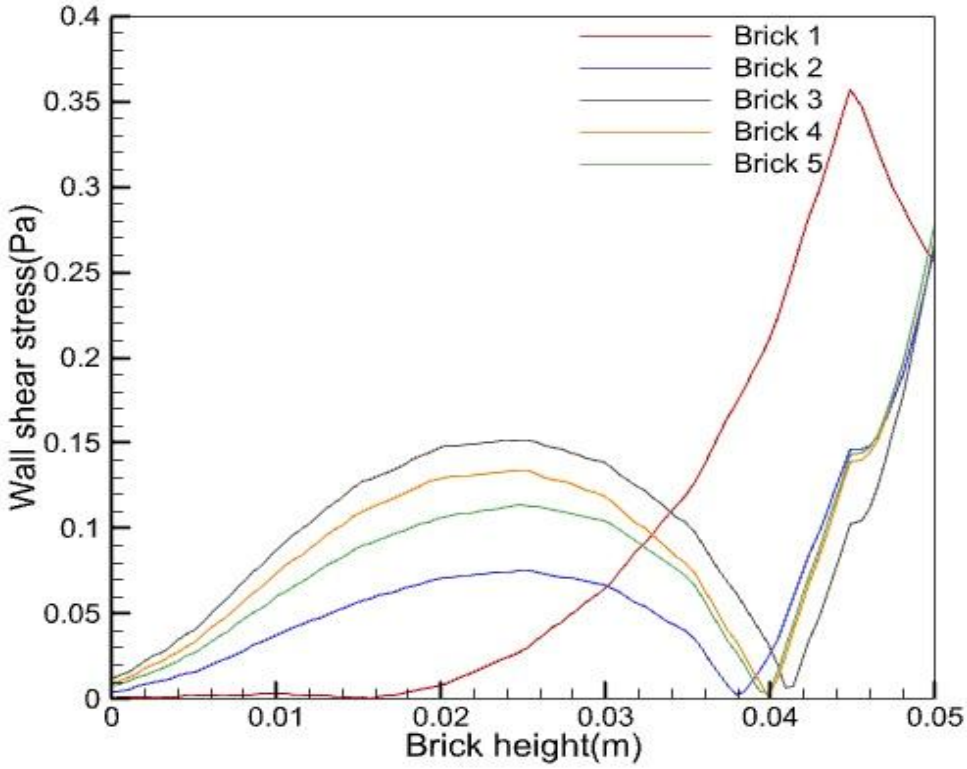

Fig. 5.8: Wall shear stress distribution for intermediate type roughness (p/k=5)

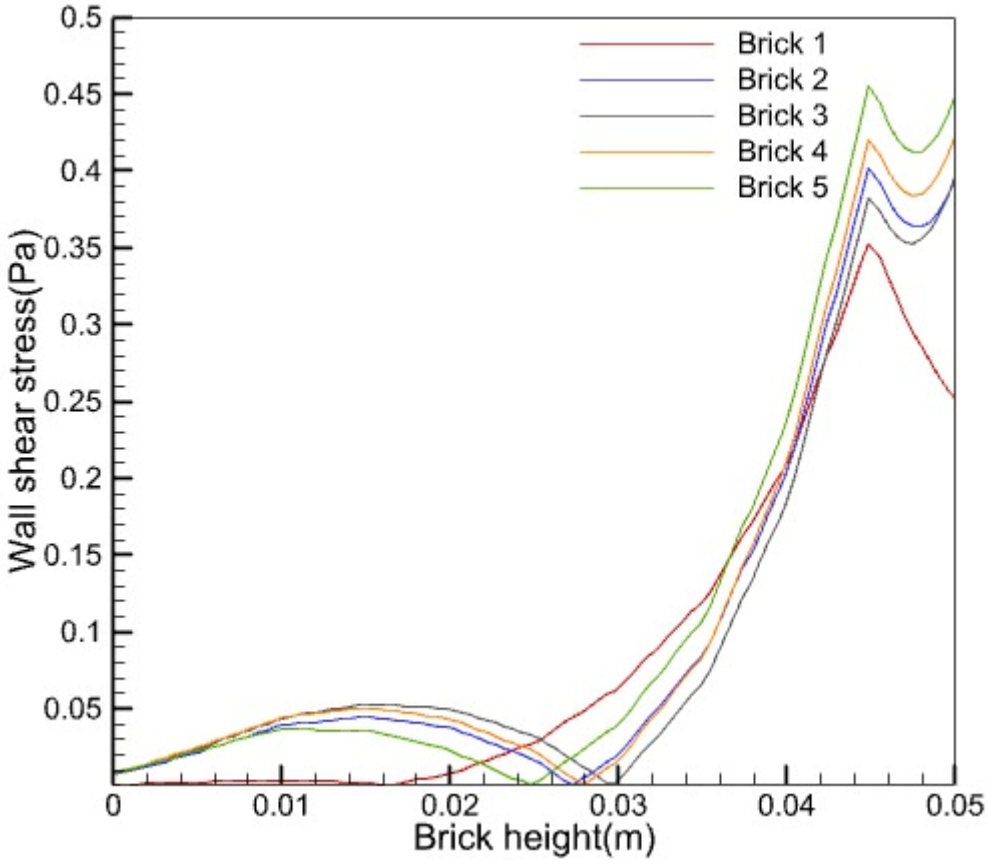

Fig. 5.9: Wall shear stress distribution for k-type roughness (p/k=9)

It is clear that a constant velocity given to the upper layer of the fluid (air) at inlet does not create much difference in the wall shear stress. The irregularity in wall shear stress is seen on the transverse face of brick 1 and brick 2 and so on. As near the corner of brick, eddy formation is taking place so wall shear stress increases at that portion and then becomes zero at the mid-point of vertical surface of brick, and then starts increasing depending on the velocity gradient.

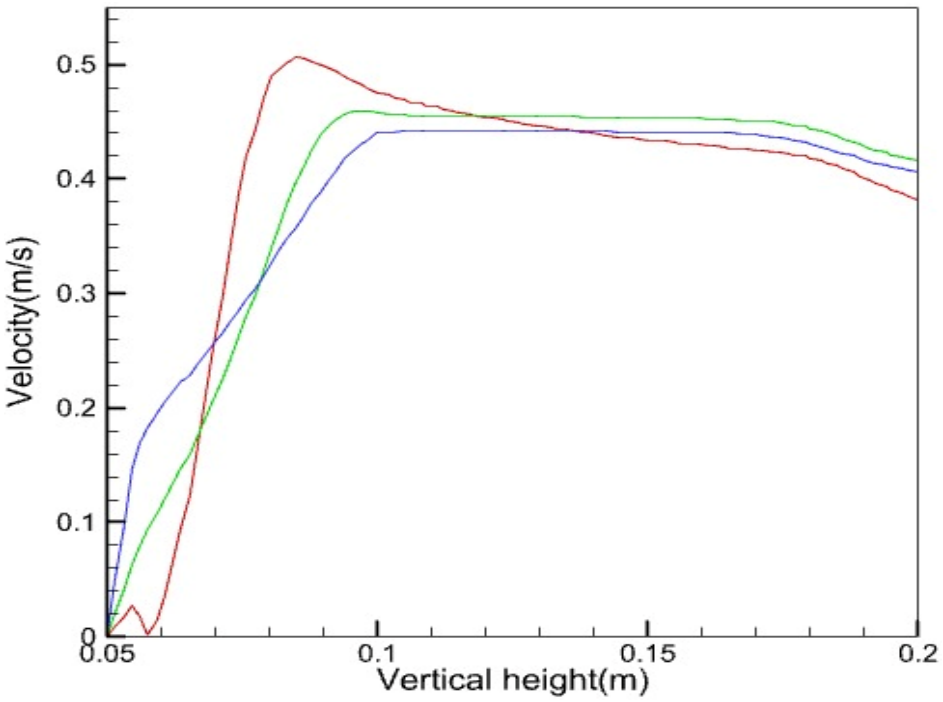

Fig. 5.10: Velocity fluctuation for d-type roughness (p/k=3)

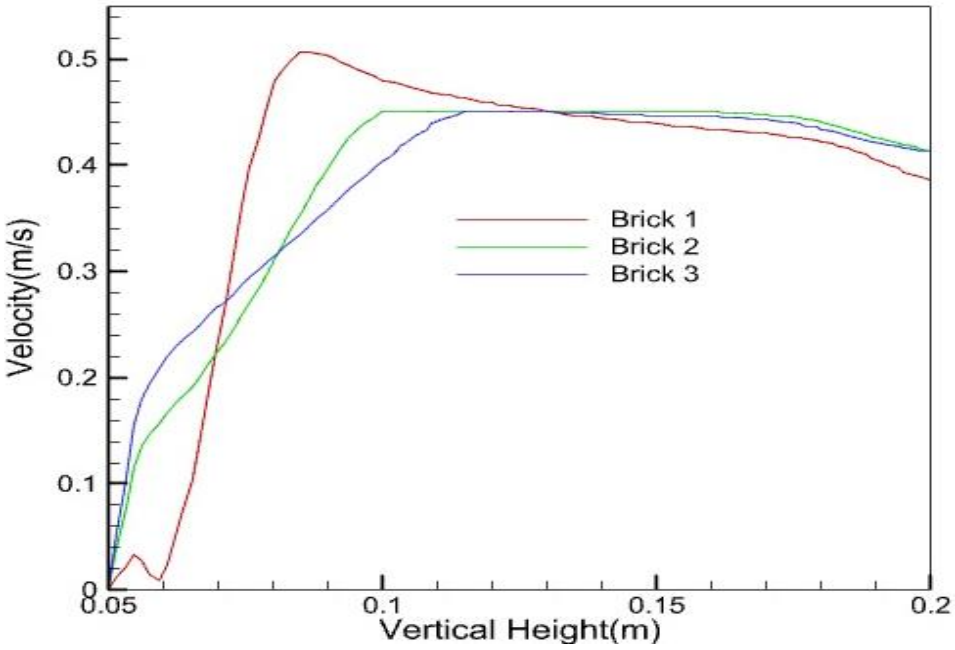

Fig. 5.11: Velocity fluctuation for intermediate type of roughness

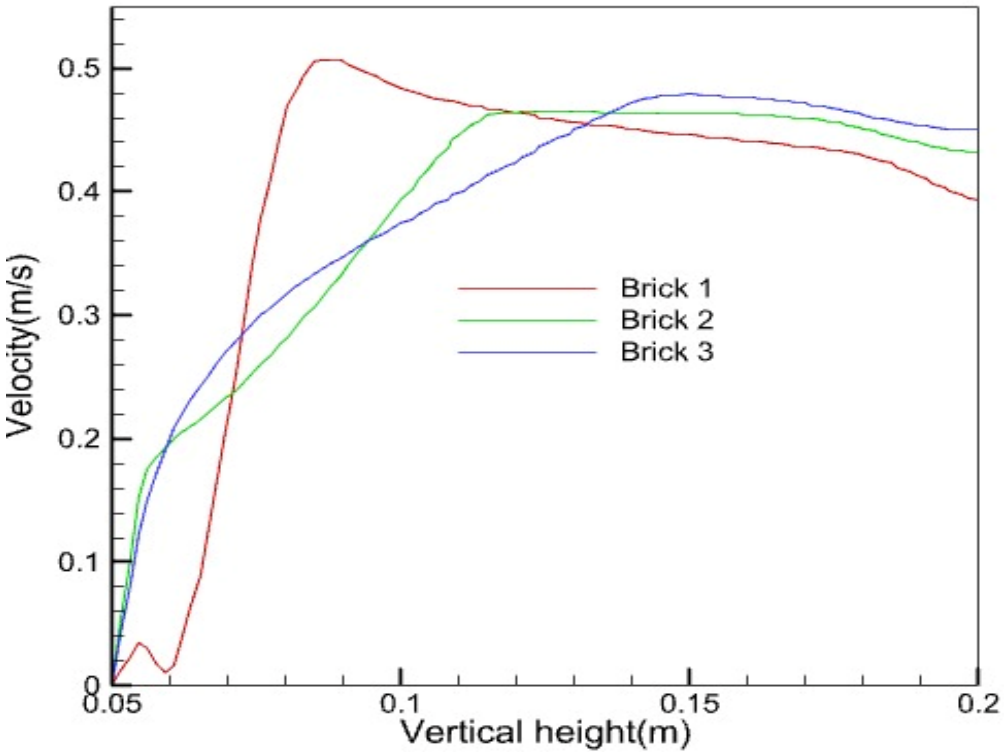

Fig. 5.12: Velocity fluctuation for k-type roughness (p/k=9)

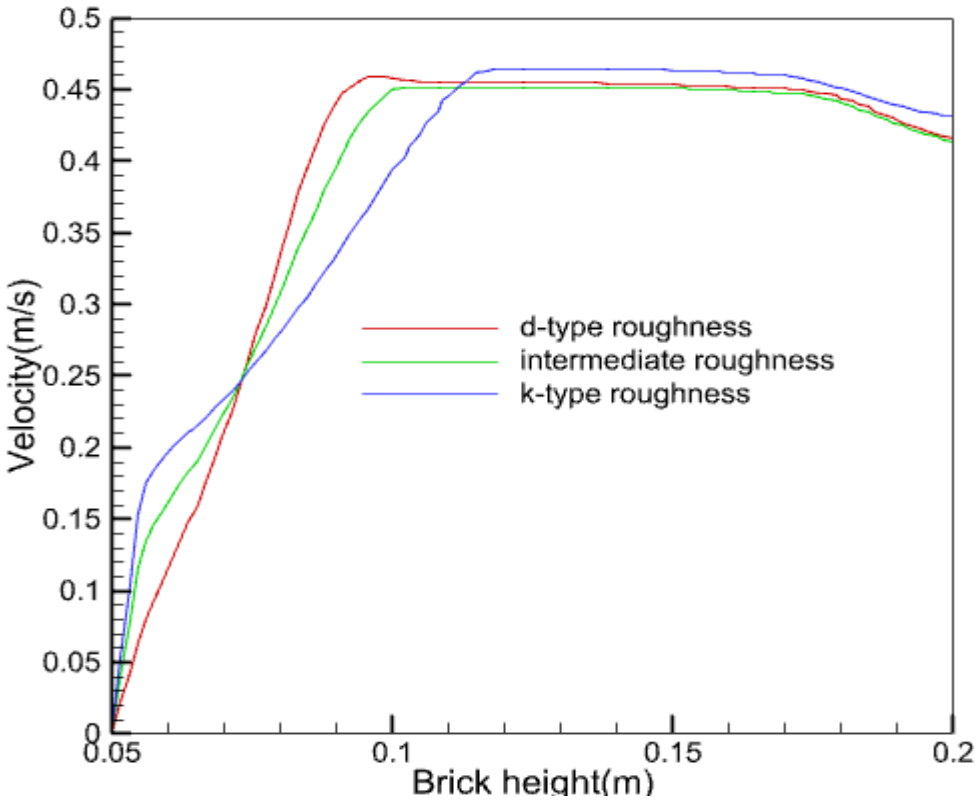

Fig. 5.13: Comparison of velocity fluctuation for different types of roughness on rib 2

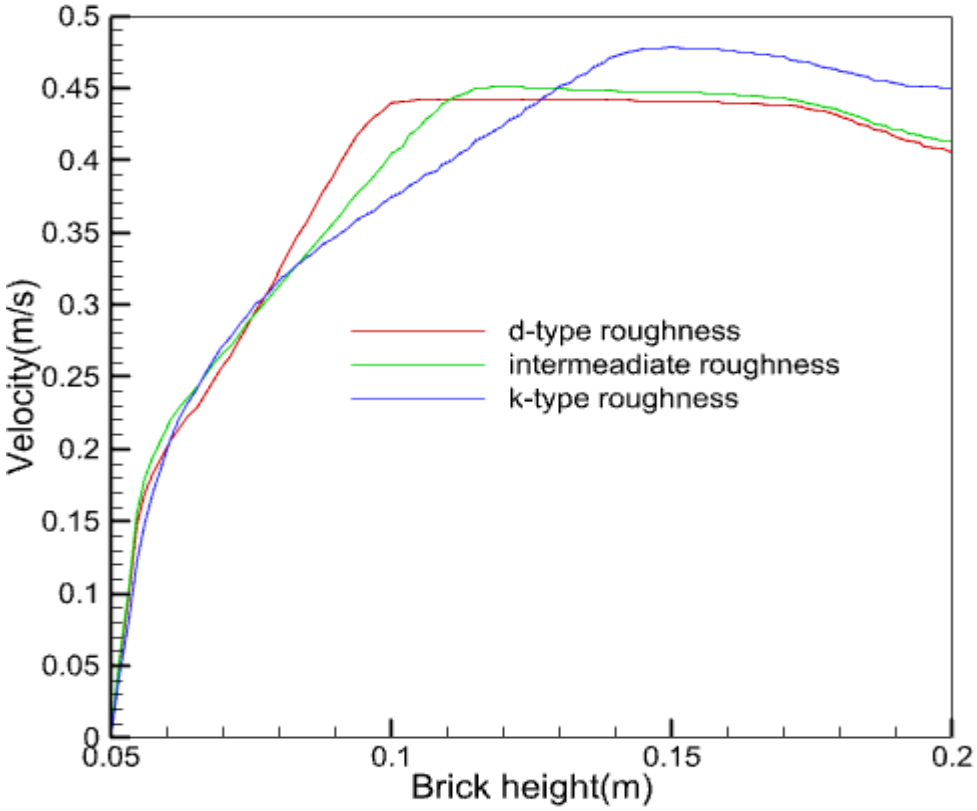

Fig. 5.14: Comparison of velocity fluctuation for different types of roughness on rib 3

Figure 5.12, 5.13, 5.14 represents the velocity fluctuation for three different types of roughness. It is seen that with depth of water, flow is nearly same as that of first case when velocity given at inlet to water only. It is seen that after hitting the brick velocity of water increases and thereafter a steady and almost constant magnitude is maintained. And the nature of graph of Reynolds number with depth of water will also be same as velocity plot because we know that $R_e = \frac{\rho v d}{\mu}$ and all the parameter is constant and only velocity is changing.

Chapter 6: Conclusion and Scope for Future work

6.1. Conclusion

In this study, a numerical modelling for multiphase flow over square ribbed surface is performed and many interesting phenomenon of the fluid has been found. An attempt has been made to investigate the effect of roughness, roughness spacing and velocity of the fluid on the fluid flow in case of an open channel whose bottom surface has a regular roughness.

In first case of the study, velocity is imposed to the lower fluid (water) and upper fluid (air) is at rest. The velocity contour and the nature of streamline indicate that when the space is less (more) in between two consecutive ribs, the velocity fluctuation and chance of eddy formation or chance of energy losses are less (more). Hence, p-type roughness has a very significant influence on the velocity dynamics and d-type has less influence. The variation of velocity has a great role in the fluid flow over a rough surface. When the velocity is less, the fluid takes entry each and every space between two consecutive ribs and chance of formation of eddy is high. Hydraulic jump is also observed very prominently in this case. The transformation of energy happens in regular manner. The spacing between two consecutive ribs and velocity of the fluid combined has a great influence in the field of open channel flow.

The variation of wall shear stress on first rib is different from the variation of wall shear stress on second and third rib due to the velocity gradient over the ribs. Wall roughness also led to higher turbulence levels in the outer region of the boundary layer. We have analysed that the position of the peak of wall shear stress greatly depends on the roughness geometry. The height at which peak stress is obtained, shifts to lower position with the increase in rib spacing i.e., decrease in roughness density.

From the nature of wall shear stress, it is established that on the first rib, maximum impact force acting is not at the corner of the rib, it is acting just below the corner of the rib. This phenomenon leads to conclude that the velocity gradient is high at that point.

There is an interesting observation from this whole study is that the nature of wall shear stress is approximately same for low inlet velocity and high p/k value.

We also concluded that the velocity given to upper layer of fluid (air) at inlet has no such influence in the flow field over the entire length of the open channel.

6.2. Scope for future work

The developed method and methodology can be used for further exploration in addition of heat, magnetic force, electromagnetic effect etc. The variation of geometry of the channel, rib and various types of roughness may be attempted to understand how the nature of flow is behaved. This can be used to create turbulence in flow. It can also be used in HVAC industry to create turbulence in duct. River morphology and ecological process such as benthic macro invertebrate drifting, bio-particle transport from mechanical perspective could be a very good scope of this study.

Reference

1. A.E. Perry, W.H. Schofield, P.N. Joubert, Rough wall turbulent boundary layers, J. Fluid Mech. 37 (2) (1969) 383–413.
2. S Nakagawa, Y Na, and TJ Hanratty. Influence of a wavy boundary on turbulence. Experiments in Fluids, 35(5):422-436, 2003.
3. Dubravka Pokrajac, Lorna Jane Campbell, Vladimir Nikora, Costantino Manes, and Ian McEwan. Quadrant analysis of persistent spatial velocity perturbations over square-bar roughness. Experiments in fluids, 42(3):413-423, 2007.
4. Cyril W Hirt and Billy D Nichols. Volume of fluid (VOF) method for the dynamics of free boundaries. Journal of computational physics, 39(1):201-225, 1981.
5. C. Manes, D. Pokrajac, I. McEwan, V. Nikora, Turbulence structure of open channel flows over permeable and impermeable beds: a comparative study, Phys. Fluids 21 (12) (2009) 125109.
6. Pankaj Kumar Raushana, Arnov Paula, Santosh Kumar Singh, Koustuv Debnatha, Spatially-averaged turbulent flow characteristics over ribbed surface in presence of unidirectional wave over steady current, Applied Ocean Research 100 (2020) 102154
7. Edgar A. C. Ferreira, Aggelos S. Dimakopoulos and Rui M. L. Ferreira, CFD MODELING OF ROUGH-BED OPEN-CHANNEL FLOWS
8. Faruque, MD Abdullah Al and Balachandar, Ram, "Effect of Reynolds Number on Wall-normal Turbulence Intensity in a Smooth and Rough Open Channel Using both Outer and Inner Scaling" (2016). International Journal of Civil, Environmental, Structural, Construction and Architectural Engineering, 10 (12), 1469-1474.
9. M. F. Tachie, D. J. Bergstrom, R. Balachandar, Rough Wall Turbulent Boundary Layers in Shallow Open Channel Flow, S0098-2202(00)00803-8
10. M. Agelinchaab, M.F. Tachie, Open channel turbulent flow over hemispherical ribs, Int. J. Heat and Fluid Flow 27 (2006) 1010–1027
11. Ludovic Cassan, Hélène Roux, Denis Dartus. Velocity distribution in open channel flow with spatially distributed roughness. Environmental Fluid Mechanics, Springer Verlag, 2019, pp.1-19. ff10.1007/s10652-019-09720-xff. ffhal-02648480
12. B. K. Gandhi, H.K. Verma, Boby Abraham, INVESTIGATION OF FLOW PROFILE IN OPEN CHANNELS USING CFD, IGHM-2010, Oct. 21-23, 2010, IIT Roorkee, India

13. Vladimir Nikora, Derek Goring, Ian McEwan, and George Griffiths, SPATIALLY AVERAGED OPEN-CHANNEL FLOW OVER ROUGH BED, J. Hydraul. Eng. 2001.127:123-133.
14. Vladimir Nikora, Ian McEwan, Stephen McLean, Stephen Coleman, Dubravka Pokrajac and Roy Walters, Double-Averaging Concept for Rough-Bed Open-Channel and Overland Flows: Theoretical Background, 10.1061/(ASCE)0733-9429(2007) 133:8(873)
15. Wen, J.; Chen, Y.; Liu, Z.; Li, M. Numerical Study on the Shear Stress Characteristics of Open-Channel Flow over Rough Beds. Water 2022, 14, 1752.
16. L. Djenidi, R. Elavarasan, R.A. Antonia, The turbulent boundary layer over transverse square cavities, J. Fluid Mech. (1999), vol. 395, pp. 271–294.
17. P.A. Krogstad and R. A. Antonia, Surface roughness effects in turbulent boundary layers, Experiments in Fluids 27 (1999) 450-460
18. P.A. Krogstad, H.I.Andersson, O.M.Bakken and A.Ashrafian, An experimental and numerical study of channel flow with rough walls, doi:10.1017/S0022112005003824
19. Jie Cui, Virendra C. Patel, Ching-Long Lin, Large-eddy simulation of turbulent flow in a channel with rib roughness, International Journal of Heat and Fluid Flow 24 (2003) 372–388.
20. Yasutaka Nagano, Hirofumi Hattori, Tomoya Houra, DNS of velocity and thermal fields in turbulent channel flow with transverse-rib roughness, International Journal of Heat and Fluid Flow 25 (2004) 393–403.
21. S. Leonardi, P. Orlandi, L. Djenidi, R.A. Antonia, Structure of turbulent channel flow with square bars on one wall, International Journal of Heat and Fluid Flow 25 (2004) 384–392.
22. Dong Hyun Lee, Dong-Ho Rhee, Kyung Min Kim, Hyung Hee Cho, Hee Koo Moon, Detailed measurement of heat/mass transfer with continuous and multiple V-shaped ribs in rectangular channel, Energy 34 (2009) 1770-1778.
23. S. E. Coleman, V. I. Nikora, S. R. McLean and E. Schlicke, Spatially Averaged Turbulent Flow over Square Ribs, DOI: 10.1061/(ASCE)0733-9399(2007)133:2(194)